Effect of nanoparticles on properties of geopolymers designed for well cementing applications

Muhammad Awais Ashfaq Alvi [*], Mahmoud Khalifeh, Mesfin Belayneh Agonafir

Dept. of Energy and Petroleum Engineering, University of Stavanger, Norway

ABSTRACT

Recently the focus of the oil and gas industry is to find the alternative material for well barrier applications. Geopolymers are among the suggested materials, which could be used in the future to solve the well integrity issues rooted by the properties of Portland cement. Previous study with rock-based geopolymer indicates the potential of geopolymer to be used as a barrier material. However, there are still some shortcomings of geopolymer material, which need to be improved to make it a possible option for well cementing applications. This study aims to improve the properties of the geopolymer. Al_2O_3 and multi walled carbon nanotubes functionalized with hydroxyl group (MWCNT-OH) nanomaterials were used to study their effect on rheological, filtration loss, and mechanical properties of the geopolymer. Moreover, the effect of nanomaterials on the setting time and microstructure of the geopolymer has been studied. Results obtained from this work indicate that, nanomaterials-based geopolymers have better mechanical properties and setting time compared to the neat geopolymer. Addition of nanomaterials produced a more ductile structure with higher compressive and tensile strengths. Microstructure and element analysis confirmed the formation of a more compact and dense structure with the presence of MWCNT-OH and Al_2O_3 throughout the structure of the geopolymer.

1. Introduction

In hydrocarbon wells, cement is one of the important well barrier elements used during well construction, completion, and Plug and Abandonment (P&A) phases. When well productivity is not economical, or the well experience uncontrolled leakage, the fate of the well is to be permanently plugged and abandoned. The primary function of well cementing is to seal annular spacing between casing-casing or casing-formation, hinder formation-casing communication, providing structural integrity, and preventing formation fluid from leaking to the surface (Nelson and Guillot, 2006). Fig. 1 presents possible leak scenarios that occurred due to improper zonal isolation. Possible leak paths from the well could be: through cement due to permeability of cement, through cracks caused by downhole stresses (e.g. thermal shocks, tectonic stresses, post-cement operations) and brittleness of cement, in the microannuli at the interface of casing-cement or cement-formation caused due to shrinkage of cement and/or insufficient wetting to ensure bonding between casing and cement. Properly designed slurry, as well as good cementing practices, are the key factors for successful cementing operation. For any civil engineering works, it is important to

follow recommended practices and standards. NORSOK D-10 (2013) defines well integrity as "*the application of a technical, operational, and organizational solution to minimize the risk of an undesired leak during the lifetime of the well.*

Well integrity issues are reported in several parts of the world. For instance, Vignes and Aadnøy (2010) have audited the integrity status of the Norwegian Continental Shelf (NCS) wells based on the information obtained from seven operators. As shown in Fig. 2, their investigation indicated that out of the 75 wells (i.e., 48 production and 27 injection wells), casing and cement integrity issues recorded 11% of well integrity issues each. A recent survey performed by the Petroleum Safety Authority (PSA) Norway on 1995 wells from 13 operators shows that 30 % of the wells have well integrity issues (Norway, 2019).

Moreover, Watson and Bachu (2009) have statistically assessed the leakage potential of several abandoned wells in Alberta, Canada. This study indicates that improper zonal isolation is one of the causes of leak to the environment.

Depending on the well design and completion, qualified cement can be counted either as a well barrier element in the primary or secondary barrier envelope (see Fig. 1). Although cement has been the prime
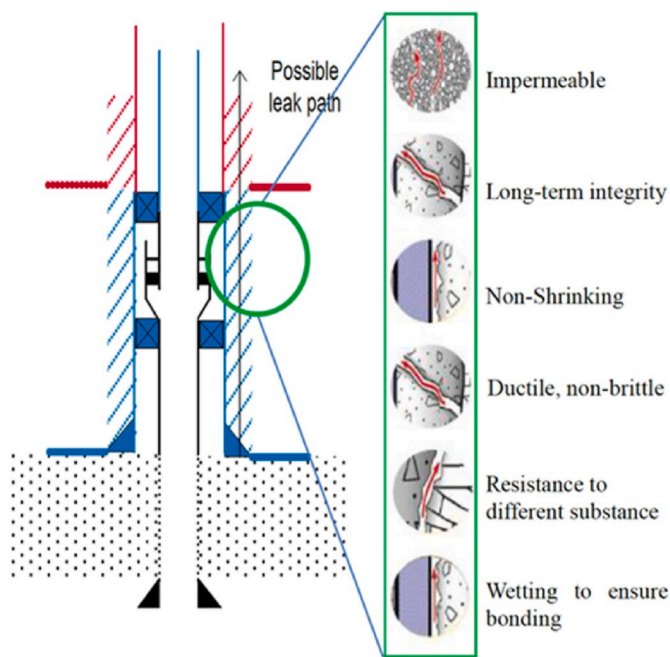

Fig. 1. Well barrier envelopes (blue as primary and red as secondary) and NORSOK D-10 cement requirement (Belayneh and Aadnøy, 2015; Norsok, 2013). (For interpretation of the references to colour in this figure legend, the reader is referred to the Web version of this article.)
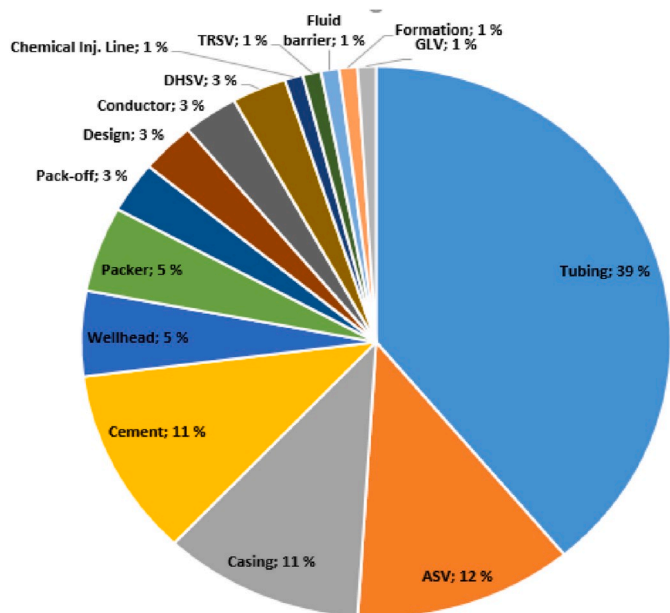

Fig. 2. Categories of well barrier element failures in the Norwegian sector of the North Sea (Vignes and Aadnøy, 2010).

material used for zonal isolation and P&A, the enacted mechanical and long-term durability requirements by different authorities make the use of alternative barrier materials important. NORSOK D-10 (2013) reminds that any barrier material used for zonal isolation or P&A shall be impermeable, able to withstand mechanical loads/impact, and non-shrinking. In addition, the candidate material shall resist downhole chemicals and ensure bonding with steel and formation. Obtained results by different researchers and dialogue with operators suggest that the use of alternative material to Portland cement might be necessary to reduce the risk of well barrier failure (Teodoriu et al., 2013; Jafariesfad

et al., 2017a; Kiran et al., 2017; Salehi et al., 2017; Vrålstad et al., 2018).

The primary failure mechanisms associated with the Portland cement are addressed as, but not limited to, changes of temperature and pressure regimes that cause cement cracks, brittleness (low ductility) of cement, volume changes causing possible microannuli (Vrålstad et al., 2018). Furthermore, poor cementing practices can result in channels through cement (Shenold and Teodoriu, 2016) and tectonic stresses (Lavrov and Torsæter, n.d; Jafariesfad et al., 2017a; Vrålstad et al., 2018) are circumstances that intensify the risk of material failure. However, due to the above shortcomings with the Portland cement, researchers are trying to look for supplementary materials. Several alternative materials such as bismuth-based materials (Carragher and Fulks, 2018), resins, creeping formation, and geopolymer have been proposed or used as an alternative to Portland cement (Khalifeh et al., 2013, 2014; Vrålstad et al., 2018).

Geopolymers have been used in the construction industry and suggested as a supplementary material to cement for well construction (Khalifeh et al., 2014, 2018; Liu et al., 2017; Salehi et al., 2019). Geopolymers are inorganic polymers made of a long chain of aluminosilicate materials formed by the process of geopolymerization. Geopolymerization is the term introduced by Joseph Davidovits in 1978 (Davidovits, 1982, 1991). In this process, reactive alumina and silica-based materials, known as precursors, act as source material. The source material is mixed with a hardener, which is an alkali silicate solution to activate the geopolymerization process. Three different mechanisms (dissolution, orientation and polycondensation) are involved during the geopolymerization process (Duxson et al., 2007; Davidovits, 2005). A variety of precursor materials based on natural minerals such as feldspar, metakaolin, kaolinite, and solid wastes like fly ash, blast furnace slag, rice husk, and several others can be used to produce geopolymers. The geopolymer structure has a 3-D network gel consisting of SiO_4 and AlO_4 tetrahedrons that are bonded alternately by sharing the oxygen ions as Si–O–Al–O (Davidovits, 2005; Komnitsas, 2011). The stability and strength of the geopolymer depend on the properties of the source material. Some of these properties may include, but not limited to, fineness, particle size distribution, chemical composition and reactive content of the geopolymeric precursors (Singh et al., 2015). Moreover, the concentration of soluble silicate, water content, and pH level of the hardener are also important factors (Duxson et al., 2007).

Different researchers studied the advantages and current limitations of geopolymers compared to conventional cement. Some of the advantages include durability at corrosive environments (Nasvi et al., 2014; Khalifeh et al., 2017), lower permeability (Gao et al., 2013; Salehi et al., 2016; Nasvi et al., 2014), higher structural flexibility (Khalifeh et al., 2015), lower chemical shrinkage (Salehi et al., 2016, 2017; Paiva et al., 2018; Khalifeh et al., 2018) and lower CO_2 emission during production (Gao et al., 2013). However, there are current limitations that limit the application of geopolymer for well construction. These include lower tensile strength compared to Portland cement and issues related to controlling the pumpability of geopolymer slurry at elevated temperature for a reasonable time (Khalifeh et al., 2018). Another main barrier is that technology has not been field tested and, therefore, not yet qualified for use.

1.1. Nanomaterials in cement and geopolymer

In recent years, research results have shown that nanomaterials (1–100 nm) can significantly improve the properties of conventional drilling fluid, oil well cement, and enhanced oil recovery processes. Nanomaterials have shown great potential to solve engineering problems related to the oil and gas industry. Due to a very small size and high surface area to volume ratio, nanomaterials have the ability to create smart materials with improved rheological and mechanical properties. For instance, the application of nanoparticles in cement has shown improved properties such as increase in compressive strength (Li et al.,

2004; Meng et al., 2012; Safi et al., 2018), flexural strength (Li et al., 2004; Safi et al., 2018), tensile strength (Jalal et al., 2012) and reduced permeability (Ozyildirim and Zegetosky, 2010). Researchers working in the areas of well cementing have also introduced nanomaterials to their mix designs to achieve better properties of the cement material (Ershadi et al., 2013; Pang et al., 2014; de Paula et al., 2014; Khan et al., 2016; Murtaza et al., 2016; Jafariesfad et al., 2017b; Li et al., 2017).

Moreover, the application of nanoparticles in geopolymer has shown impacts on different properties. Many studies are available which show the impact of nanoparticles on workability (Hassaan et al., 2015; Phoo-ngernkham et al., 2014; Rodríguez et al., 2013; Gao et al., 2014), microstructure (Assaedi et al., 2016; Phoo-ngernkham et al., 2014), chemical shrinkage (Yang et al., 2015) and density and porosity (Deb et al., 2016; Assaedi et al., 2015, 2016). Additionally, the effect of nanoparticles on the mechanical properties of geopolymers has been studied by some authors (Assaedi et al., 2016; Phoo-ngernkham et al., 2014; Naskar and Chakraborty, 2016). However, very few studies are available to address the effect of nanoparticles on the properties of geopolymers for oil well cementing (Ridha and Yerikania, 2015; Khalifeh et al., 2019a,b).

In geopolymer technology, the presence of aluminium oxide plays an important role. By decreasing the ratio of Si/Al, the final geopolymer material can be more flexible with a higher degree of resistivity to corrosive chemicals (Provis and Van Deventer, 2009). In addition, the use of aluminium for producing lightweight and sound-isolating geopolymers have been studied by some researchers (Hajimohammadi et al., 2017; Leiva et al., 2019). We also know that the hydroxyl group plays a role in the geopolymerization reaction. Therefore, the use of nanoparticles functionalized with OH^- involves the nanoparticles in geopolymer reactions to further enhance the properties of geopolymers.

In this study, MWCNT functionalized with a hydroxyl group (MWCNT-OH), and Al_2O_3 nanoparticles (AL-0450) have been used to study their effect on the properties of rock-based geopolymer. The impact of Al_2O_3 nanoparticles and MWCNT on different geopolymer systems have been previously studied. For instance, Guo et al. (2014) have added $\gamma\text{-}Al_2O_3$ to fly-ash based geopolymer. This study shows that Al_2O_3 nanoparticles have modified the pore structure of the geopolymer and produced a material structure with a narrow pore distribution based on the FT-IR spectrum and SEM analysis. Also, nanoparticles improved the compressive strength of the fly ash-based geopolymer, 2.0 wt% of Al_2O_3 nanomaterials increase the strength from 50 MPa to 56.8 MPa for neat geopolymer after 28 days. Another study shows that the addition of Al_2O_3 nanoparticles to high calcium fly-ash based geopolymer decrease the setting time of the slurry (Chindaprasirt et al., 2012). Phoo-ngernkham et al. (2014) showed that the microstructure of the Al_2O_3 based high calcium fly ash geopolymer was improved, with the formation of denser structure. Additionally, nanoparticles improved elastic modulus, compressive, and flexural strength of the geopolymer paste.

MWCNTs have also been used in geopolymers to improve mechanical properties (i.e. compressive and tensile strengths as well as Young modulus) because of the superior mechanical properties of carbon nanotubes. Saafi et al. (2013) introduced MWCNT to a low calcium fly ash-based geopolymer. The addition of MWCNT having a concentration of up to 1 wt% by weight of the geopolymer improved flexural strength and Young modulus of the geopolymer. However, Saafi et al. (2013) reported that a lower concentration of the MWCNT in the geopolymer matrix gave better results due to sufficient dispersion of the nanotubes in the slurry. The effect of carbon nanotubes on the compressive strength and modulus of elasticity of fly ash-based geopolymer has been reported by Rovnaník et al. (2016). According to Rovnaník et al. (2016), the best result for compressive strength and modulus of elasticity of the geopolymer obtained when low concentration (0.15 wt%) of MWCNT was used in the mix. Published results by Abbasi et al. (2016) show that carbon nanotubes improve the strength of metakaolin-based geopolymers. According to them, an addition of 0.5% nanotubes had increased compressive strength by 32% and flexural strength by 28% of

the geopolymer. Moreover, SEM analysis confirmed the bonding of MWCNT with the geopolymer, as nanotubes bridged the microcracks in the structure of the geopolymer.

One important criterion to be considered in the selection of nanoparticles is to obtain sufficient dispersion. Agglomeration of nanomaterials may lead to a negative impact on the properties of geopolymer or other cement-based materials. Furthermore, lower concentration of nanomaterials has a better performance compared to the use of large amounts, which ultimately may lead to non-reacted nanoparticles in the cement-based materials (Guo et al., 2014; Riahi and Nazari, 2012; Sumesh et al., 2017; Khater and Abd El Gawaad, 2016).

In this paper, the intent is to study the effects of the AL-0450 and MWNCT-OH nanoparticles on rheological properties, static fluid loss, pumping time, and mechanical properties of a neat rock-based geopolymer (GP). The mechanical, elastic, and physical properties are used to quantify and analyze the quality of cementitious material. In an oil and gas well, cement can experience compressive and tensile loads. Hence, in this paper, the elastic properties of geopolymers are characterized through the uniaxial and Brazilian (indirect tensile) tests. Additionally, the microstructure of the geopolymers containing the nanoparticles was examined.

2. Experimental procedures

2.1. Materials

Granite is an intrusive igneous rock, and its main constituents are quartz and alkali feldspars. Granite was used as geopolymer precursor, in this work, to produce rock-based geopolymer. Velde Pukk AS provided powdered granite, and it was used without any further processing. The particle size of powder granite was below 63 μm. To achieve the required chemical composition of geopolymeric precursors, the chemical composition of granite was normalized by introducing silica flour and ground granulated blast furnace slag. The chemical composition of the geopolymeric precursor is presented in Table 1. The development of the rock-based geopolymer and its reaction is extensively presented in work done by Khalifeh et al. (2016).

Ground Granulated Blast Furnace Slag (GGBFS) is an industrial byproduct of the steel industry. The GGBFS has calcium and magnesium content, but the precursor mix is designed so that the final calcium content is less than 10 wt%. The GGBFS used in this study was supplied by MEROX, Sweden, with the product name Merit 5000.

Silica flour is natural quartz sand, and it was supplied by Halliburton. It was introduced to the mix design to adjust the Si/K_2O ratio.

In this research work, a potassium silicate solution was used as a hardener, which had a modulus number (SiO_2/K_2O) of 2.30. Deionized water was used to adjust the water content of the binder. The chosen nanoparticles were introduced to the binder prior to the addition of precursor.

To this liquid phase, suitable amounts of AL-0450 and MWCNT-OH were added. Nanomaterials in the liquid phase (aqueous) were used in this study. As nanomaterials are dispersions in the water phase, liquid to solid ratio of the geopolymer slurry was adjusted according to the liquid content of the nanomaterials.

2.1.1. Nanomaterials

MWCNT-OH used in this study were purchased from US Research Nanomaterials, Inc. Functionalization of MWCNT is done to improve their properties such as better dispersion, interfacial bonding strength, better flexibility as well as better surface activity. Hydroxyl functionalized nanotubes were used in this study to achieve possible reaction with the geopolymer. In addition, a non-ionic surfactant containing aromatic groups without having Alkylphenol Ethoxylates (APEO) is used to disperse MWCNT in water. Ultra-sonication and centrifugation were used to disperse the tubes and to form a stable dispersion of MWCNT in water. Properties of MWCNT-OH are presented in Table 2.

Table 1
Chemical composition of the geopolymeric precursor.

Chemical composition	SiO$_2$	Al$_2$O$_3$	Fe$_2$O$_3$	CaO	MgO	Na$_2$O	K$_2$O	TiO$_2$	MnO	SrO	BaO	S2-	LOI	Total
Wt. %	65.77	10.04	0.58	11.98	6.37	1.89	1.78	0.91	0.01	0.01	0.01	0.48	0.17	99.99

AL-0450 was purchased from the Alfa Aesar. AL-0450 is a colloidal dispersion in 50% H$_2$O with dispersant, see Table 3 for properties of AL-0450. Fig. 3 shows SEM images of the nanomaterials used in this study.

2.2. Test methods and preparation of test specimens

2.2.1. Characterization and test methods

Temperature and Pressure Conditions – For this study, the temperature was chosen to be 50 °C and 70 °C. The ramp-up rate of 1 °C/min was selected for both cases. Additionally, curing pressure used for pressurized consistency, uniaxial compressive strength, as well as ultrasonic cement analyser was 14 MPa. This was done to mimic the possible downhole temperature and pressure conditions in a well.

Shear Stress Measurement – Fann viscometer was employed to measure the rheological behaviour of the geopolymeric slurries. Atmospheric consistometer was used to do the conditioning of the geopolymer slurry at 50 °C. After reaching 50 °C, the slurry was conditioned for 20 min to achieve uniform temperature.

Consistency – In order to map pumpability and effect of pressure on the pumpability of the slurries, atmospheric consistometer and pressurized consistometer recommended by API RP 10B-2 standard (API, 2013) were employed.

Static Fluid Loss – To measure the fluid loss of the slurries; first the slurries were conditioned in the atmospheric consistometer at 50 °C (BHCT). Then, high temperature and high pressure (HTHP) fluid loss cell was used to measure the drained fluid. The achieved differential pressure was 5.2 MPa. As the slurry was already conditioned at 50 °C, the ambient temperature was used during the measurement, and all the slurries were passed through the 850 μm sieve. The pressure was applied by using carbon dioxide cartridges.

Uniaxial Compressive Strength – To measure the unconfined compressive strength of the samples, a Toni Technik-H mechanical tester was used. A loading rate of 27.6 MPa/min was selected according to the API RP 10B-2 standard (API, 2013). All the samples were cured in an autoclave at 14 MPa and 70 °C. Samples were cured in plastic cylinders having dimensions of 100 mm length and 52 mm diameter. After curing for the required time, samples were removed from the plastic molds and were cut from both ends to achieve flat surfaces before measuring the compressive strength. The specimen is loaded between parallel plates, and the loading is on the surface of the cylindrical geopolymer plug. The testing procedure is according to NS-EN 196-1 standard (Norway, 2005; ASTM, 2013), and the compressive strength is given by:

$$\sigma_c = \frac{F}{\pi R^2} \tag{1}$$

Table 2
Properties of MWCNT-OH

Properties	Values
Purity	>95 wt% (carbon nanotubes)
	>97 wt% (carbon content)
Content of –OH	1.76 wt%
Outside diameter	20–30 nm
Inside diameter	5–10 nm
Length	10–30 μm
Specific surface area (SSA)	>110 m^2/g
Color	Black
Electrical conductivity	>100 s/cm
Tap density	0.28 g/cm^3
True density	~2.1 g/cm^3

Table 3
Properties of AL-0450.

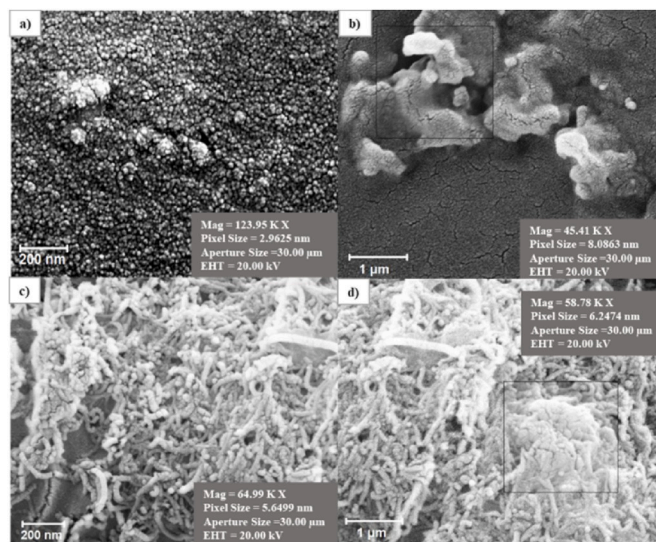| Properties	Values
Purity	50% in water, colloidal dispersion
Formula	Al$_2$O$_3$
Form	45 nm APS for dry powder
Formula Weight	101.96
Surface Area	32–40 m^2/g
Refractive Index	1.768
Color	White

Fig. 3. SEM images of AL-0450 NPs showing the distribution of nanoparticles (a and b), SEM images of MWCNT-OH showing the nanotubes (c and d).

Where F is maximum recorded compressive load (kN) and R is radius of the specimen (mm).

Indirect Tensile Strength Measurement – Brazilian tests were conducted by employing Zwick/Z020 mechanical testing machine. TestXpertII software was used to record the applied force on the sample. The loading rate of 50 N/s, which is equivalent to 0.05 MPa/s was selected according to the ASTM D3967-16 (Standard, n.d.). Unlike steel materials, rock and cement like structures exhibit weak tensile strength. Hence, the indirect test method is used to determine the tensile strength of such materials. The Brazilian tensile tests were conducted according to the procedure described in NS-EN 12390–6:2009 standard (Norway, 2009). The specimen is placed between parallel curved plates, and the applied load is continuously increased until failure. The tensile strength is given as (Norway, 2005; ASTM, 2013):

$$\sigma_t = \frac{2F}{\pi DL} \tag{2}$$

Where F is the maximum load (Newton), D is the diameter (mm), and L is the length of the specimen (mm). The unit of the tensile strength is N/mm^2.

Sonic Strength Development – Sonic Strength of the geopolymers mixed with the nanoparticles were measured by Chandler Ultrasonic Cement Analyser (UCA). The downhole temperature of 70 °C was used

to map the sonic strength development. UCAs are designed to compute the sonic strength of Portland cement by applying a pre-defined algorithm and using the travel time of ultrasound through the cement slurry. Therefore, to estimate the values for new materials, it is necessary to develop a new algorithm. For this study, a customized algorithm feature was used from UCA to accommodate geopolymer-based slurries. A polynomial equation generated from the plot between transit time and measured compressive strength from UCS was put into the UCA software using a custom algorithm option in the instrument to calculate the sonic compressive strength.

X-ray diffraction (XRD) – Bruker D8 ADVANCE Eco diffractometer (having Cu-Kα radiation source, λ = 1.5406 Å, 40 kV, and 25 mA) was used to study the X-Ray diffraction of the geopolymer and geopolymer with nanomaterials. The X-Ray patterns were recorded in the 2θ range of 5–70°.

Microstructure and Elemental Analysis – To get an insight into internal structural make-up of the geopolymer, Zeiss Supra 35VP model scanning electron microscope was used. Additionally, to quantify the percentage of different elements present in the structure, the elemental analysis was conducted with element dispersion spectra (EDS).

2.2.2. Slurry preparation

Slurry mix designs are presented in Tables 4 and 5. First, the pulverized granite rock was normalized with other industrial wastes to prepare a unique chemical composition, which gives repeatable results. Separately the hardener was prepared by mixing potassium silicate solutions with deionized water. Then, suitable amounts of either AL-0450 or MWCNT-OH were added to the hardener and mixed with a high shear rate mixer. The normalized geopolymeric precursors were mixed with the nanoparticle blended hardener by using the commercial Waring blender according to the API RP 10B-2 (API, 2013). The slurries were conditioned with the atmospheric consistometer to make sure that the system is homogenous. The sample preparations were conducted according to the API RP 10B-2 (API, 2013). The liquid to solid ratio (L/S) of the samples was 0.55. The specimens for compressive strength and tensile strength measurements were poured in the plastic molds.

3. Results and discussions

3.1. Rheological properties

3.1.1. Shear Stress Measurement

The rheological properties of the neat geopolymer show non-Newtonian (Bingham Plastic) behaviour as indicated by the previous study. The addition of nanomaterials shows similar trends but with the higher shear stress values for the same shear rate. Hence, nanomaterials increase the viscosity of the material, see Fig. 4. As indicated by Hodne et al. (2001) addition of micro-sized silica particles increased the viscosity of the cement slurry. A similar trend is observed in this study; the addition of nanoparticles to the slurry increases the solid content.

A sharp change in the rheological profile of the mix design containing MWCNT-OH was noticed at high shear rate when the temperature increased from 40 to 50 °C. The reason for the behaviour remained unknown. However, shear rates of more than 250 1/s are not commonly experienced in the field, except the Bottom Hole Assembly (Saasen and Ytrehus, 2018). Fig. 5 shows the apparent viscosity of the slurries at different temperatures. It can be seen that nanoparticles have increased the apparent viscosity. Moreover, for all the slurries increase in temperature decreases the apparent viscosities.

The Casson model is a two parameter model, which was used to

Table 4
Composition of the AL-0450 modified geopolymer.

Component	Precursor	Hardener	Water	Nanomaterials (AL-0450)
Weight (g)	735	324.45	81.9	0.36

Table 5
Composition of the MWCNT-OH modified geopolymer.

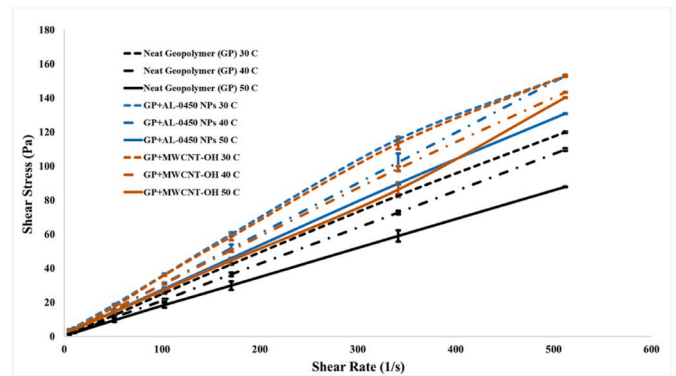| Component	Precursor	Hardener	Water	Nanomaterials (MWCNT-OH)
Weight (g)	735	324.45	81.9	0.18

Fig. 4. Effect of temperature and the nanoparticles on the rheological behaviour of geopolymer.
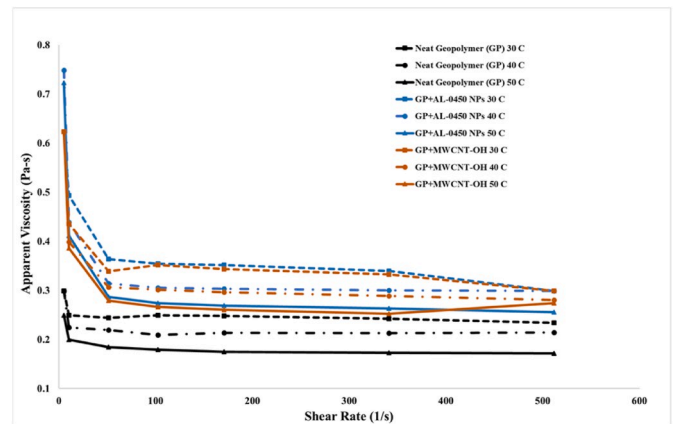

Fig. 5. Apparent viscosity of neat geopolymer and neat geopolymer modified with AL-0450 and MWCNT-OH.

calculate the Casson yield stress and Casson plastic viscosity. The Casson model provided a good fit for the measured shear stress and shear strain values. At both high and low shear rates, the Casson model provides more accurate results (Ochoa, 2006). The model is given (Nelson and Guillot, 2006) as,

$$\tau^{0.5} = \tau_c^{0.5} + \mu_c^{0.5}\gamma^{0.5} \quad \text{For } \tau < \tau_c \tag{3}$$

$$\gamma = 0 \quad \text{For } \tau \geq \tau_c \tag{4}$$

Where,

τ is the shear stress (Pa)
τ_c is the Casson yield stress (Pa)
μ_c is the Casson plastic viscosity (Pa)
γ is the shear rate (sec^{-1})

Table 6 shows the values for yield stress and plastic viscosity for neat geopolymer and geopolymer mixes having nanomaterials. Yield stress and plastic viscosity of cement-based materials are critical with respect to displacement and the pumpability of the slurry. Higher values of yield stress and plastic viscosity of the geopolymer mix with nanomaterial

Table 6
Casson Yield stresses and Casson plastic viscosities.

Temperature (°C)	Casson Yield Stress-Neat Geopolymer (Pa)	Casson Plastic Viscosity-Neat Geopolymer (Pa)	Casson Yield Stress-GP + AL-0450 (Pa)	Plastic Viscosity-GP + AL-0450 (Pa)	Casson Yield Stress- GP + MWCNT-OH (Pa)	Plastic Viscosity-GP + MWCNT-OH (Pa)
30	0.015	0.23	0.36	0.29	0.25	0.29
40	0.009	0.21	0.22	0.27	0.21	0.26
50	0.014	0.17	0.34	0.23	0.15	0.24

thickens the system and control the segregation of materials by providing better cohesion. This increase in viscosity does not have effect on the pumpability of the slurry, as indicated by the setting time results, but it can have an impact on pump pressures and friction in the well, causing larger downhole pressures when circulating.

3.2. Fluid-loss test

Fluid-loss values for cement slurries are generally high when additives are not used, which can contribute to problems such as gas migration as well as maintaining the hydrostatic pressure and incomplete hydration of cement. Geopolymerization does not involve hydration reaction and requires less amount of water, but hardener loss may result in loss of hydrostatic pressure or incomplete reaction. Our measurements confirmed that lower values of fluid loss are associated with the geopolymer. As shown in Fig. 6, very low values of fluid loss were recorded after 30 min. The mix containing AL-0450 nanoparticles showed a significant increase in fluid loss values. The possible reason might be a delay in the hardening of slurry with AL-0450, as indicated in Fig. 7. However, in the case of MWCNT-OH, there is a significant decrease in fluid loss values. Perhaps, attachment of MWNCT particles to the oligomers is a possible scenario.

3.3. Pumpability

For oilfield applications, geopolymeric slurry should set at the desired time. Therefore, it is crucial to have control over the setting time of the slurry. Retarders (such as lignosulfonates, and derivatives of carbohydrate) are commonly used to delay the setting time of Portland cement used in oil fields. However, these are not effective in case of the geopolymers. Borax based retarders are suggested for the geopolymer; however, a significant decrease in mechanical strength has been reported (Allouche et al., 2017). Therefore, nanomaterials might be used to prolong the pumpability of the geopolymer slurries by acting as a retarder. Fig. 7 shows that the addition of nanomaterials almost doubles the available pumping time of the geopolymers. Different mechanisms could be involved here, which causes the delay in the setting of

Fig. 6. Effect of AL-0450 nanoparticles and MWCNT-OH on static fluid loss of the geopolymeric slurries.

nanomaterials-based geopolymer slurries. A possible scenario could be that the nanomaterials might act as a shield between the aluminosilicate precursor and hardener and reduce the rate of dissolution of alumina-silicates (Allouche et al., 2017).

Delaying the gelation step can significantly prolong the setting of the geopolymer slurry. As with the addition of nanoparticles, there are more charged particles in the system, the electrostatic repulsion between the similar charges in the system may be promoted. Also, surfactants that are used to disperse the nanoparticles might act as retarders and delay the setting time of the geopolymer slurries. The addition of the nanomaterials prolonged the pumping time to 3 hrs, see Fig. 7.

Our study shows that pressure does not have a significant effect on pumping time, see Fig. 7, which is aligned with previous results obtained by Khalifeh et al. (2019a) on the neat geopolymers.

3.4. Mechanical properties

3.4.1. Uniaxial compressive strength (UCS)

The unconfined compressive strength tests were performed after the specimens being aged at 12hr, 24hr, 3, 7, and 28 days. For each curing time, three specimens were crushed, and the average strength values are reported as a representative for the unconfined compressive strength. Even though the geopolymer specimens were cured in autoclaves, the mechanical destructive tests were conducted at ambient conditions. Fig. 9 shows a continuous increase in the strength development of geopolymers with the incorporation of MWCNT-OH and AL-0450 NPs. This shows that nanoparticles are integrated into the material structure. As indicated in Fig. 9, there is not a very significant difference between the compressive strength between 7 days and 28 days. This indicates that samples attained most of the strength in the first 7 days. However, there is a continuous increase in strength with time. Introducing nanomaterials to the geopolymeric slurry might provide additional nucleation sites for the aluminosilicate reaction, forming a more homogeneous and denser geopolymer paste. Narrow pore distribution and elimination of weaker zones within the geopolymer matrices could lead to an increase in compressive strength. Hydroxyl groups on the surface of the MWCNT may either react with the geopolymer structure and releasing a hydroxyl group or make a hydrogen bond, as illustrated in Fig. 8. This incorporates the MWCNT throughout the structure of the geopolymer, as indicated by the microstructure analysis. It can ultimately produce nanotubes reinforced geopolymer having higher mechanical properties such as compressive strength. Li et al. (2013) have shown that the incorporation of Carboxymethyl chitosan improves the mechanical properties of the fly ash-based geopolymer due to the created hydrogen bond between the hydroxyl groups in N-Carboxymethyl chitosan and the geopolymer.

In case of AL-0450 NPs, the smaller size of these particles may also act as a filler and fill the pores in the structure of the geopolymer, consequently yielding a more compact structure.

3.4.2. Stress and strain curves

Fig. 10 shows the measured stress-strain. As shown, the nanoparticle treated system exhibited a longer deformation as well as a higher load carrying capacity depending on the curing time. All the geopolymer samples showed creeping behaviour, which means more ductility. However, it is important to mention here that this behaviour is dependent on the curing time, as indicated in Fig. 10, after 28 days
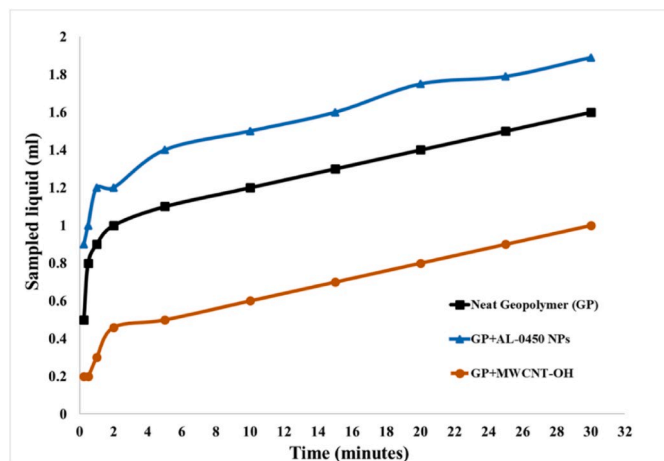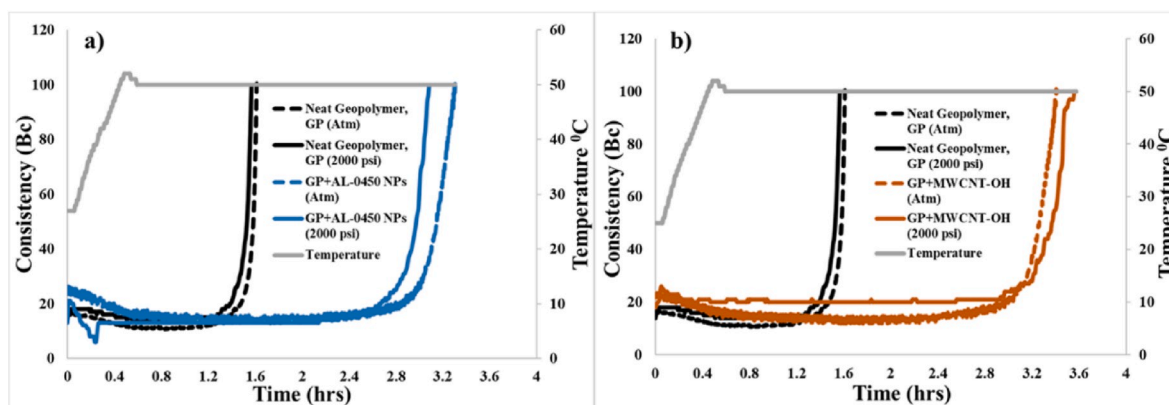
Fig. 7. a) Effect of AL-0450 nanoparticles on setting time of the geopolymer slurry b) Effect of MWCNT-OH on setting time of the geopolymer slurry.
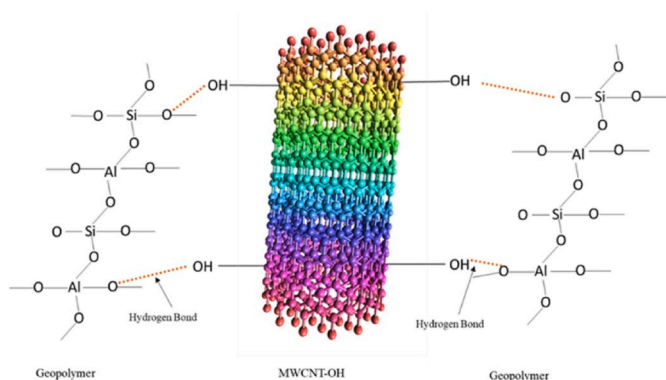

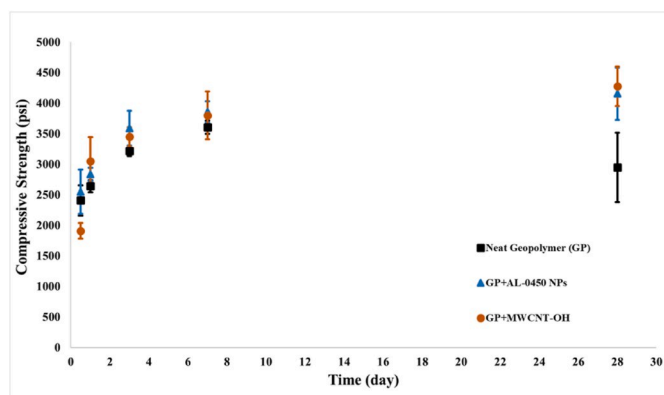**Fig. 8.** Hydrogen bond formation between MWCNT-OH and geopolymer.

Fig. 9. Trend for unconfined compressive strength build up from 12 h to 28 days for neat geopolymer, and modified geopolymers with nanomaterials AL-0450 and MWCNT-OH.

nanomaterials-based system because less ductile with the time.

3.4.3. Modulus of elasticity

Tensile strength requirements for the oil well cement are dependent on Young's modulus (E) of cement and formation rock (Thiercelin et al., 1998; Williams et al., 2011). Downhole stresses caused by temperature or pressure changes, throughout the well life-cycle, can result in the failure of cement sheath integrity (De Andrade and Sangesland, 2016). Thiercelin et al. (1998) stated that higher compressive and tensile strengths are not always the solution, and the flexibility of cement is required in several cases to minimize the damage. Due to limitations to use tri-axial cell, the piston displacement measurements, from uniaxial

compressive strength measurement, were used to study the elasticity. Although the estimated values are lower than real elasticity, the relative elasticities still remain comparable. As shown in Fig. 11, the introduction of nanomaterials to geopolymers did not significantly increase Young's modulus of the geopolymers. After 28 days, there is a minor increase in Young's modulus values, which is because of an increase in the unconfined compressive strength of the nanomaterials based geopolymers. In fact, higher compressive strength and tensile strength with low Young's modulus are beneficial for oil well cementing applications. The flexibility of the MWCNT-OH based geopolymer is expected to be due to a flexible nanotube structure. Also, functionalization with the –OH groups incorporate more flexibility in the structure of the geopolymer. In case of AL-0450, there is a sharp increase in the Young modulus values in the first 3 days. This is due to the higher unconfined compressive strength achieved by this sample in the first 3 days. As shown in Fig. 9, AL-0450 based system attained most of his strength in 3 days, and afterward, there is a slow increase in the strength.

3.4.4. Compressive strength to young modulus ratios

Increase in the ratio of unconfined compressive strength to Young's modulus values for the nanomaterials based geopolymer indicates that nanomaterials-based system has higher compressive strength with lower values for Young's modulus. A decrease in the value after 28 days is due to an increase in both compressive strength and Young's modulus. However, for nanomaterials-based system, the ratio is slightly better than the neat geopolymer, see Fig. 12.

3.4.5. Tensile strength (TS)

As geopolymers are known to possess lower values of tensile strength, it is vital to improve their tensile strength for well cementing applications. Nanomaterials used in this work have improved the tensile strength of the neat geopolymer until 7 days. AL-0450 and MWCNT-OH have significantly improved the tensile strength for 7 days; the latter has even more effect on the tensile strength (see Fig. 13). The MWCNT–OH additive improved the tensile strength of the geopolymer by 123% while the AL-0450 additive leads to a 68% improvement for 7 days. Higher tensile strength of the modified geopolymers with nanomaterials make them more stable against tensile failures. However, for longer curing time, the increase in the tensile strength is not very significant compared to the neat geopolymer. After 28 days, mixtures with nano-additives showed a decrease in tensile strength values compared to 7 days. However, in the case of MWCNT-OH, tensile strength values are still better compared to neat geopolymer after 28 days, see Fig. 13. It is important to mention here, that new batch of materials was used for 28 days tensile strength, therefore this could be the reason of lower values compared to 7 days test.
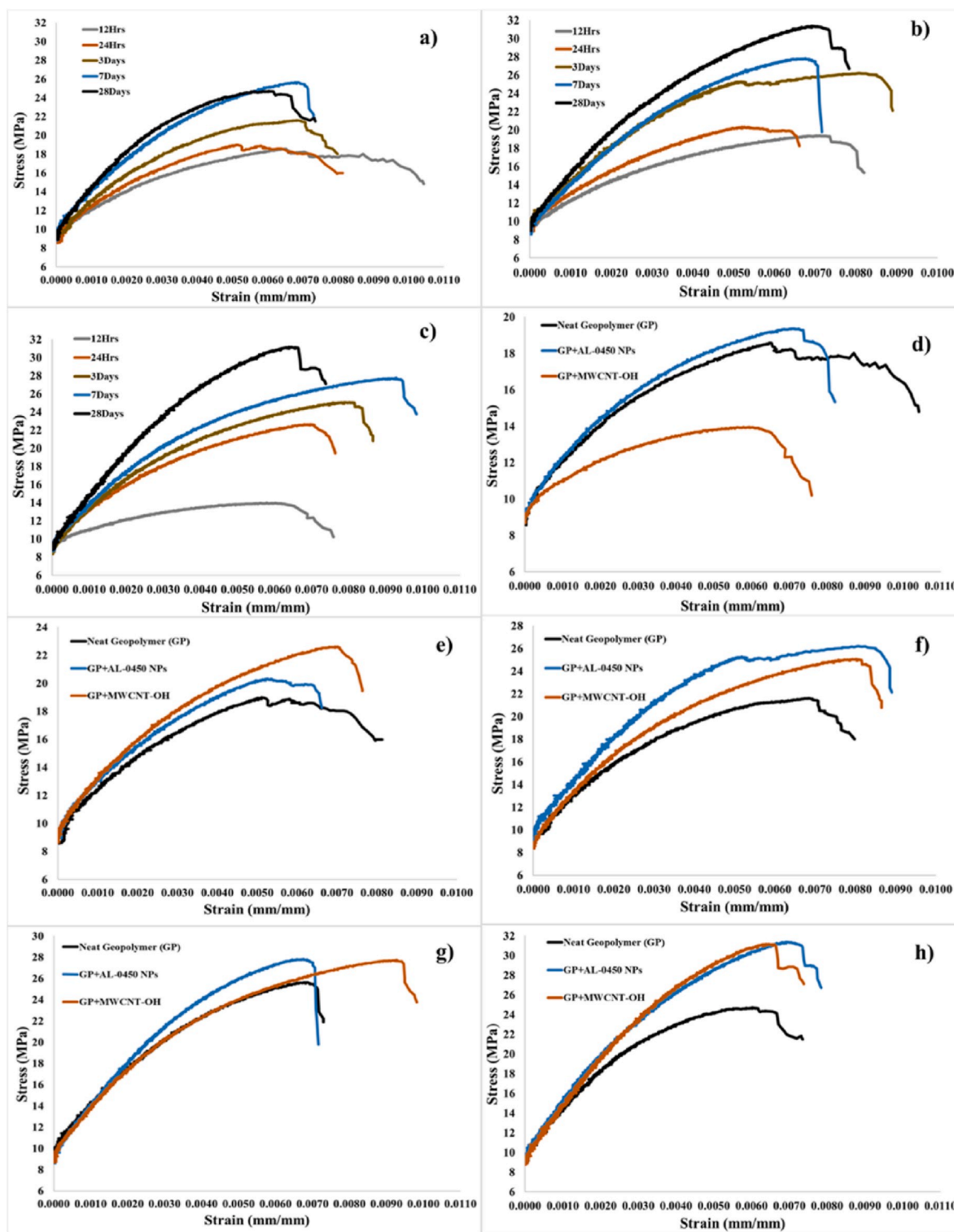
Fig. 10. Strain vs Stress curves of samples cured at different days; 70 °C and 14.7 MPa a) Neat geopolymer b) Neat geopolymer and nano AL-0450 modified c) Neat geopolymer and nano MWCNT-OH modified d) Comparison of Neat geopolymer with AL-0450 and MWCNT-OH modified geopolymer after 12 hrs e) Comparison of Neat geopolymer with AL-0450 and MWCNT-OH modified geopolymer after 24 hrs f) Comparison of Neat geopolymer with AL-0450 and MWCNT-OH modified geopolymer after 3 days g) Comparison of Neat geopolymer with AL-0450 and MWCNT-OH modified geopolymer after 7 days h) Comparison of Neat geopolymer with AL-0450 and MWCNT-OH modified geopolymer after 28 days.

3.4.6. Tensile strength to Young's modulus ratios

There is a significant increase in the ratio of tensile strength to Young's modulus for the rock-based geopolymer modified with the nanomaterials for 7 days (see Fig. 14). This substantial increase, especially in case of MWCNT-OH, could be attributed to the high tensile strength of the nanomaterials formulated geopolymer slurry. At the same time, Young's modulus is relatively low. In order to minimize the mechanical damage to the cement sheath, it is beneficial to have a high strength to Young's modulus ratio (Roy-Delage et al., 2000). However, after 28 days, the increase is not very significant compared to the neat
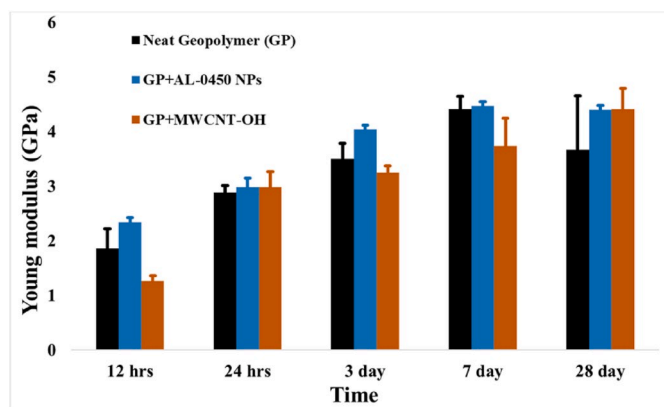
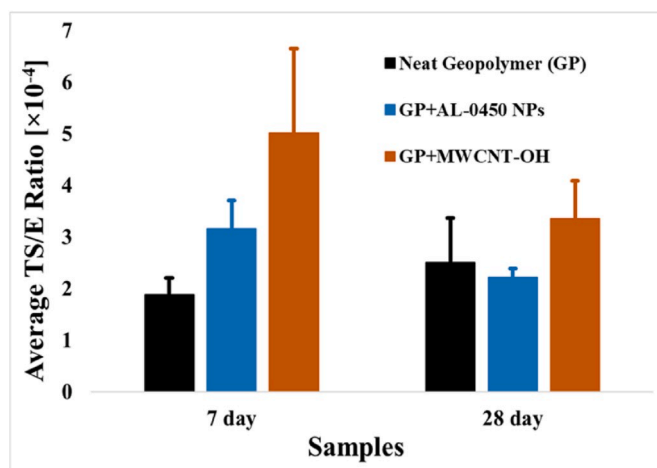**Fig. 11.** Estimated Young's modulus values for neat geopolymer, nano AL-0450 and MWCNT-OH modified geopolymers.
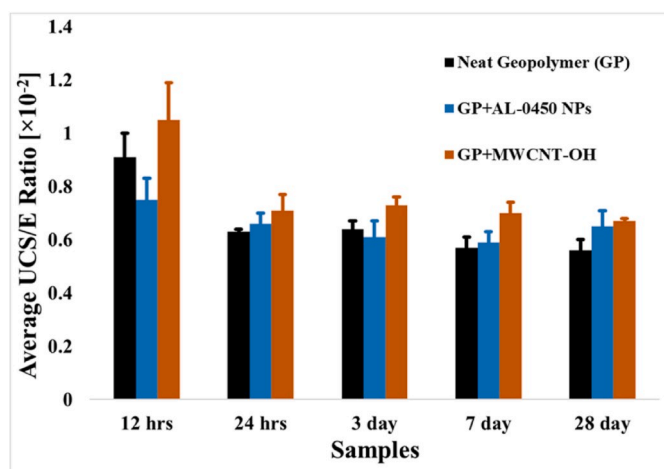

Fig. 12. Ratio of unconfined compressive strength to Young's modulus at different curing time.
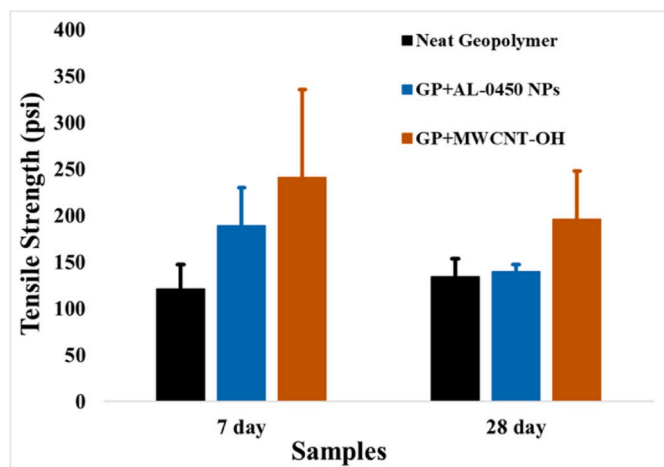

Fig. 13. Indirect tensile strength of the samples cured at 70 °C and 14.7 MPa.

geopolymer. In case of AL-0450, there is a slight decrease in ratio compared to the neat geopolymer, while for MWCNT-OH, the ratio still showed improvement.

Fig. 14. Ratio of average tensile strength to Young's modulus of the samples.

3.5. Sonic strength

Table 7 shows the empirical correlation developed in this study to be used for estimating the sonic strength development of the geopolymers and geopolymers modified with nanomaterials. The sonic strength measurements show that the maximum strength development occurs on the first day. A comparison of the UCA and consistency results show that the geopolymers set a little faster in static conditions compared to the dynamic situation (compare Figs. 7 and 15). It could be due to a delay in gelation caused by a continuous mixing of the slurry. High values of transit time at the start are due to the ramp-up of the temperature to 70 °C, which reduces the viscosity of the slurry as also shown in Figs. 4 and 5 that high temperature decreases the viscosity of the slurries (Panchmatia et al., 2019). Moreover, additives used could also affect the ultrasonic wave transmission, which can influence the transit time (Liu, 2017).

3.6. X-ray diffraction

X-ray analysis of the neat geopolymer and geopolymer with nanomaterials is shown in Fig. 16. XRD pattern of neat geopolymer showed that quartz (SiO_2), albite $Na(AlSi_3O_8)$, microcline ($K(AlSi_3O_8)$), illite ($K_{0.65}Al_{2.0}[Al_{0.65}Si_{3.35}O_{10}](OH)_2$) and clinoptilolite-Na ((Na,K,Ca)$_{2-3}Al_3(Al,Si)_2Si_{13}O_{36}\cdot12H_2O$) are the main phases present in the geopolymer structure. Minor peaks for oligoclase ((Ca,Na)$(Al,Si)_4O_8$) are also present.

Similar phases are also present in the nanomaterials based geopolymer structures. Fig. 17a–d shows that additional peaks are present for geopolymer with AL-0450. For instance, peak at 8.75° is due to the formation of phyllosilicates minerals from mica group like phlogopite ($KMg_3(AlSi_3)O_{10}(OH)_2$). Small peaks at 9.9, 11.1°, and 13-14° are due to the formation of zeolite-based mineral (e.g. clinoptilolite-Na and albite). Moreover, smaller additional peaks at 19-20° for geopolymer having AL-0450 additive are due to the formation of illite. Peaks present at 21-25° are due to the formation of albite, microcline, oligoclase, and illite. The broad peak at 26° is due to quartz, there is a minor shift in the peak for geopolymer with AL-0450 due to the formation of microcline and albite, and an additional peak at 26.7° is for microcline.

Table 7
Empirical Correlations obtained from the plot between uniaxial compressive strength and Transit time.

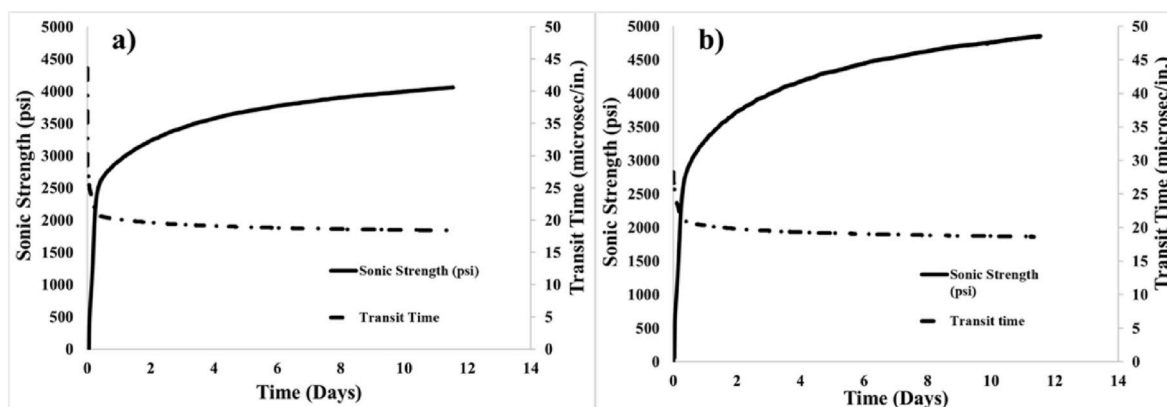| Samples	Empirical Correlation
GP + AL-0450	$y = 27.658x^2 - 1775.7x + 27797$
GP + MWCNT-OH	$y = 66.938x^2 - 3583.8x + 47808$

Fig. 15. a) Sonic Strength development of geopolymers modified with nano AL-0450 b) Geopolymers modified with nano MWCNT-OH.
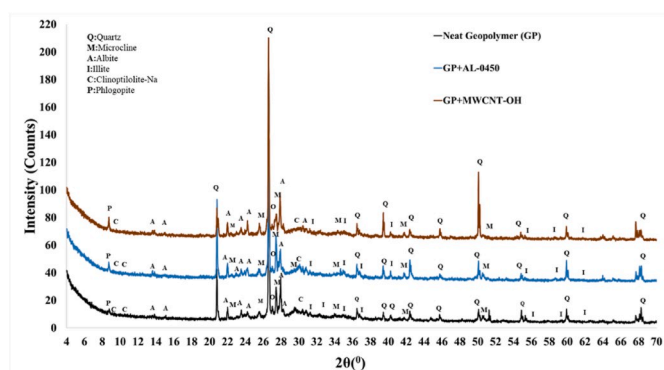

Fig. 16. XRD pattern for the neat geopolymer and geopolymer with AL-0450 NPs and MWCNT-OH.

Similar to neat geopolymer, peaks at 27-33° are due to albite, illite, and microcline phases with few additional peaks for the same phases for geopolymer with AL-0450. New peaks at 34.64° are formed due to the formation of almandine (Fe$_3$Al$_2$(SiO$_4$)$_3$). Also, there are minor peaks for alumino-magnesiotaramite (Na(CaNa)(Mg$_3$Al$_2$)(Si$_6$Al$_2$)O$_{22}$(OH)$_2$) at 34-35°. A peak at 41.8° is for diaspore (AlO(OH)) for a geopolymer with AL-0450.

There are also additional peaks for berlinite (AlPO$_4$) at 20.9–26.6° and 34-68°, specifically at 64.1–67.9°. The sharp peak at 60.08° is due to the formation of mullite (3Al$_2$O$_3$.2SiO$_2$). Moreover, additional albite, illite, and microcline are also present throughout 30-70° for geopolymer with AL-0450 additive.

The additional sharp peak at 8.75° is also present for MWCNT-OH due to the formation of phyllosilicates minerals. In case of MWCNT-OH geopolymer, the broad peak around 13.6° is associated with graphite, while other peaks are due to additional aluminosilicate minerals like albite. In addition, the carbon peak is formed at 20.96° for MWCNT-OH. There is a peak shift for MWCNT-OH at 26° is due to the graphite peak at 25.60° is overlapping with a quartz peak. There is also a broad peak at around 27.44° because of graphite for MWCNT-OH. Additional peaks for MWCNT-OH at 28.2° is due to microcline. A peak at 39.5° is due to the formation of albite and illite. Minor peaks at 42.3, 42.5, and 44.6° are due to graphite. In addition, minor peaks at 54-55° are also due to graphite. X-ray analysis indicates that additional phases are formed in case of geopolymer slurries with nano-additives. It shows that nanoparticles took part in the reaction. The stability of nano-materials dispersion might be the reason for the effective reaction between nano-additive and other raw materials used to formulate geopolymer slurries. Moreover, in case of MWCNT-OH, the hydroxyl groups might be a possible reason for taking part in the reaction, see

Fig. 8.

3.7. Microstructure analysis

Microstructure analysis shows that nanomaterials have reacted with the geopolymer components and contributed in the geopolymerization. As shown in Fig. 19 a-d, the AL-0450 nanoparticles based geopolymer has form dense microstructure as compared to the neat geopolymer, see Fig. 18 a-d. Nanomaterials are able to form a structure that is more compact and improved interlocking morphology, as shown in Fig. 19 d). AL-0450 nanoparticles produced highly ordered geopolymer structure, as revealed in Fig. 19, due to the low ratio of Si/Al. Yong et al. (2007) have observed similar behaviour where a decrease in Si/Al ratio contributed to higher chemical interactions and a more ordered structure. Studies have indicated that nanomaterials fill the gaps in the structure of a geopolymer, which constructed a more homogenous and compact structure (Huang and Han, 2011; Lo et al., 2017). In addition, this structure produced materials with higher strength, as confirmed by the compressive strength results.

Similarly, for MWCNT-OH based geopolymer, the nanotubes have reacted with the geopolymer and produced a structure that is more compact without any pores and empty spaces in the structure. As mentioned previously in the introduction that MWCNT bonded the surfaces of the geopolymer and uniformly distributed in the geopolymer structure as indicated in Fig. 20 b. Moreover, nanotubes bridged the microcracks in the structure of the geopolymer. Since the samples used for the SEM analysis are from the compressive strength test, therefore there are cracks in the structures as indicated by the SEM images.

3.7.1. EDX analysis

Fig. 21 shows the elemental analysis for the neat geopolymer, and it can be seen that a lower amount of aluminium is present in the neat geopolymer. Additionally, carbon is not present in the geopolymer without MWCNT-OH.

EDX analysis for the geopolymer with nanomaterials showed that both AL-0450 and MWCNT-OH contributed to the geopolymerization reactions. As shown in Figs. 22 and 23, both AL-0450 and MWCNT-OH are uniformly distributed throughout the structure of the geopolymer. Stable dispersions of nanoparticles in dispersants may be contributed to this phenomenon. The uniform distribution of nanomaterials is critical to improve the properties of the geopolymer. Mapping of the geopolymer structure with AL-0450 and MWCNT-OH also indicates that addition nanoparticles increase the percentage of aluminum and carbon respectively in the geopolymer structure.

Testing results performed in this work indicates the potential of nano-additives in altering properties of geopolymer mixtures. Rheology results showed that nanomaterials could increase the viscosity of the slurries, however for both neat geopolymer slurries and slurries with
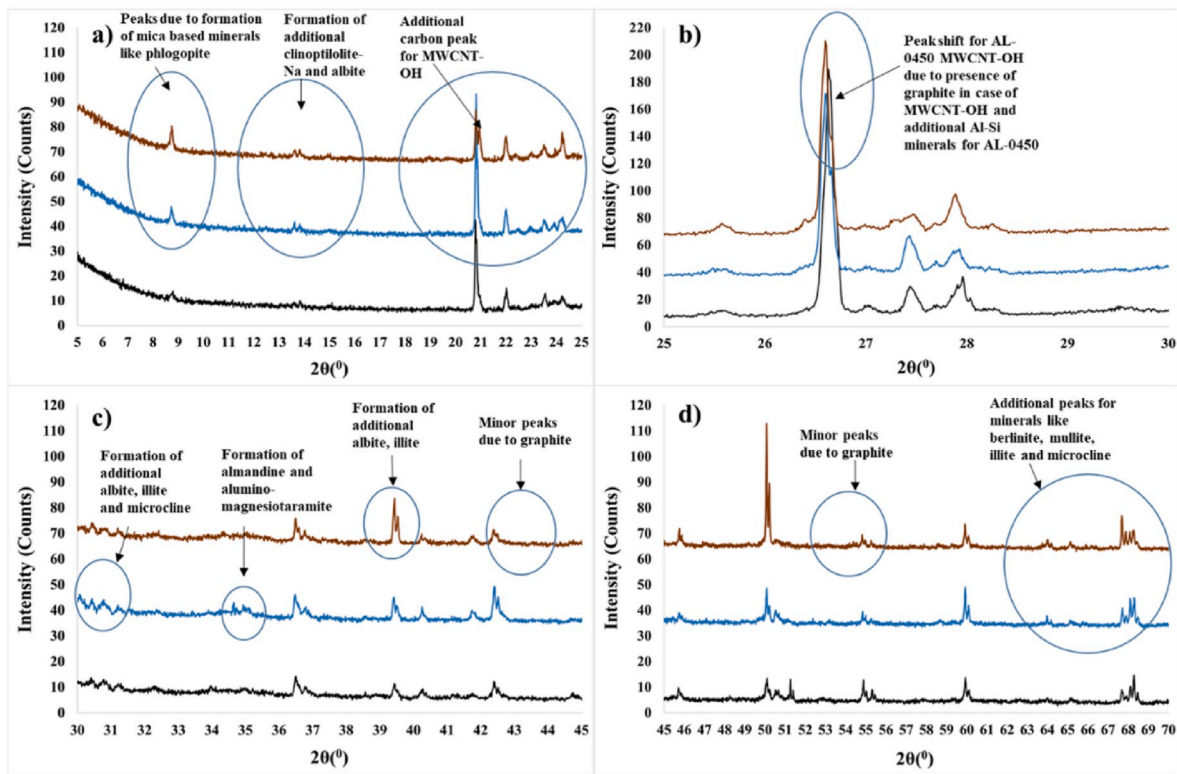
Fig. 17. (a–d) XRD pattern for the neat geopolymer and geopolymer with AL-0450 NPs and MWCNT-OH indicating additional peaks and peak shifts for geopolymer with nanomaterials.
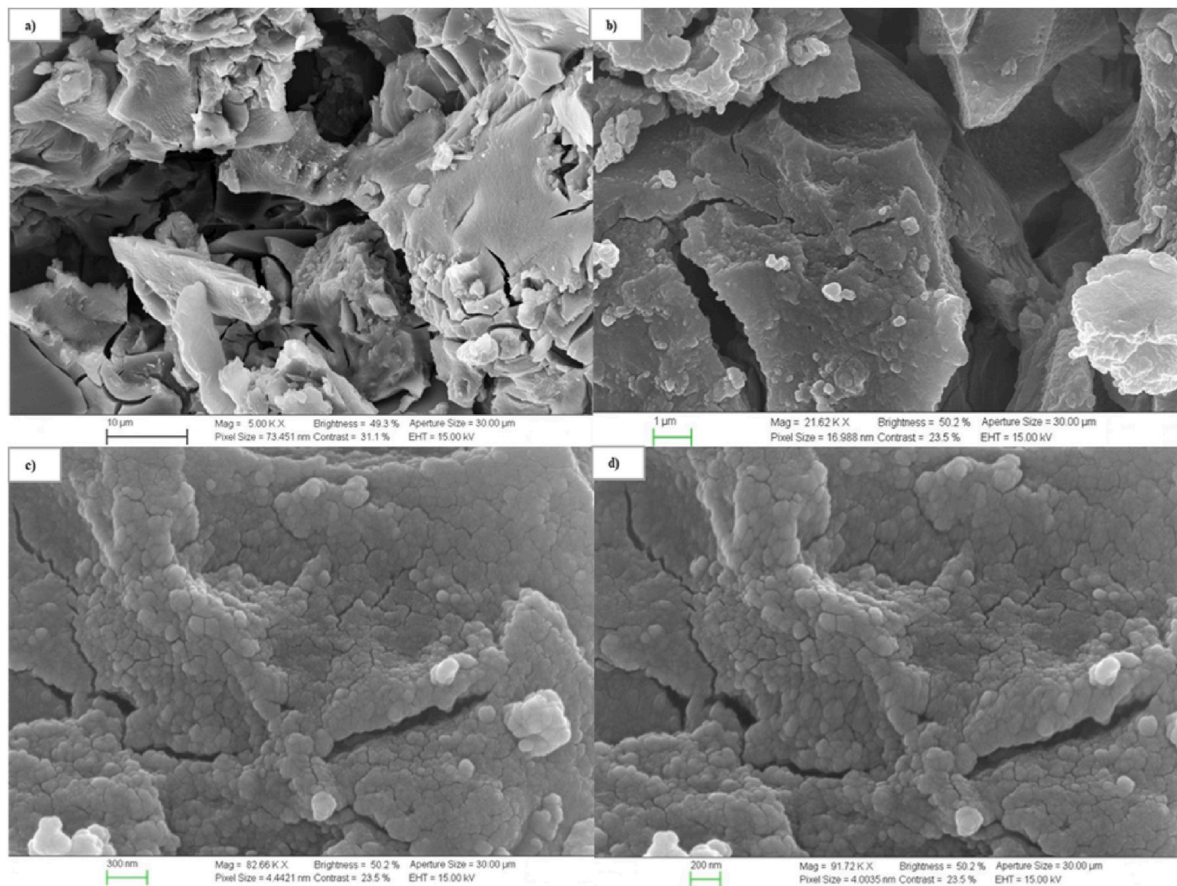

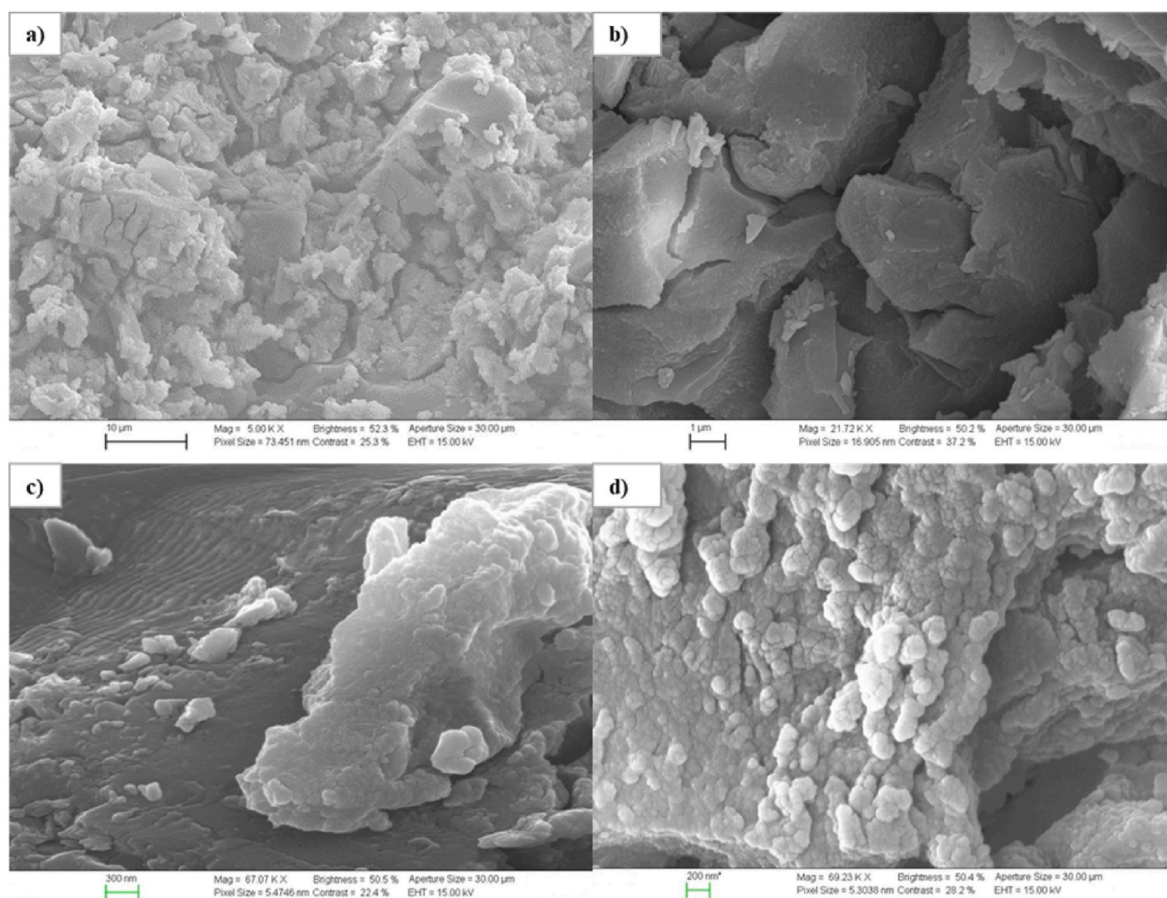**Fig. 18.** SEM images of the neat geopolymer.

Fig. 19. SEM images of geopolymer with AL-0450 NPs a) overview of the structure b) Internal structure showing AL-0450 NPs and geopolymer c) AL-0450 NPs presence in the structure of geopolymer d) Compact structure of geopolymer with AL-0450 NPs.

nano-additives, viscosity decreased with temperature. Moreover, nano-additives also increase the plastic viscosity, apparent viscosity, and yield point of the geopolymer. However, as indicated in Fig. 7 an increase in viscosity does not have effect on pumpability. Also, the fluid loss result in Fig. 6 showed that geopolymer having AL-0450 nanoparticles have more fluid loss, which might be due to delay in the setting of the slurry. While in the case of MWCNT-OH, delay in setting did not affect the fluid loss and, in fact, improved the fluid loss compared to neat geopolymer. It could be explained from Fig. 8, which suggests the attachment of MWCNT-OH with the oligomers. The attachment of tube structures with the geopolymer structure controls the loss of fluid.

Fig. 7 showed the ability of nano additives to delay the setting of geopolymers, additionally setting time of slurries is not affected by pressure, and as slurries with nano-additives took almost the same time to set under atmospheric and high pressure. Unconfined compressive strength results showed that nano-additives could improve the compressive strength of neat geopolymer. The geopolymer achieves most of the strength in the first 3 days, see Figs. 9 and 15. After 3 days, there is a steady increase in the compressive strength values, and there is not a very significant difference between 7 and 28 days. Therefore, no test was performed for 14 days. However, it would be interesting to check in the future how the materials behave after 14 days. Stress-strain curves in Fig. 10 indicates that until 7 days nanomaterials-based slurries showed longer deformation and higher load carrying capacities. While, as curing time increases, mixtures with nanomaterials become less ductile, which indicates that materials could become more brittle with the time. Fig. 11 also confirms this phenomenon where Young's modulus of the geopolymer mixture with nanomaterials is higher than neat geopolymer, which suggests that mixtures with nanomaterials become less ductile after 28 days. This could be disadvantage for long-term

wellbore integrity. However, Fig. 12 indicates that the ratio of UCS and Young's modulus for the mixtures with nanomaterials after 28 days is slightly better than the neat geopolymer. Moreover, Fig. 10 h also showed that mixtures with nanomaterials still showed higher load carrying capacity and reasonable deformation compared to the neat geopolymer. Future study with curing samples for 6 months can provide the answer if nanomaterials-based mixture becomes more brittle or not.

Tensile strength results indicate that nanomaterials have improved the tensile strength of neat geopolymer for 7 days. However, after 28 days, mixtures with nanomaterials showed lower tensile strength values compared to 7 days. It indicates that for longer period nanomaterials based geopolymers lost their tensile strength. However, further studies are needed to find the reason for these phenomena and to confirm that nanomaterials might not improve the strength of neat geopolymer for longer periods.

Sections 3.5 to 3.7 are the test performed to compliment the tests in the previous section. Sonic strength result showed that reduction in viscosity causes the transit time to increases, which supports the reduction in viscosity with temperature, as indicated in Fig. 15. Also, this test supports that mixtures attained most of their strength during the early stages of curing. X-ray analysis, SEM, and EDX analysis confirms the involvement of nanomaterials during geopolymerization.

New minerals formation, as indicated by X-ray analysis, confirms the presence of nanomaterials in the mixture. SEM analysis shows the compact structure formation for the geopolymer mixtures with nanomaterials. Which, also indicates that nanomaterials are well mixed with precursor and other raw materials used to formulate geopolymer. EDX results conformed the uniform distribution of the elements present in the nanomaterials, which again confirms the proper reaction between nano additives dispersions and other additives used to formulate geopolymer
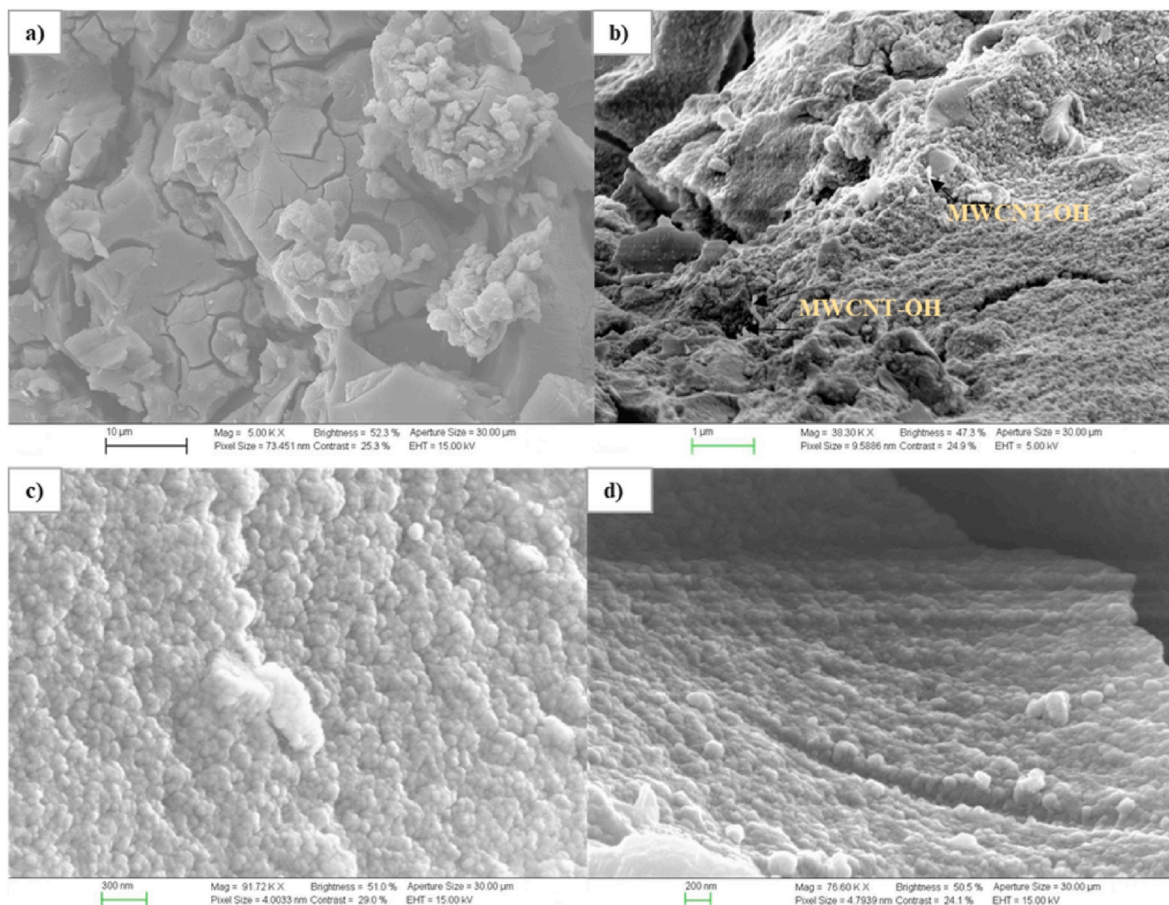
Fig. 20. SEM images of Geopolymer with MWCNT-OH a) overview of the structure b) Internal structure showing MWCNT-OH and geopolymer c) MWCNT-OH presence in the structure of geopolymer d) Compact structure of geopolymer with MWCNT-OH.
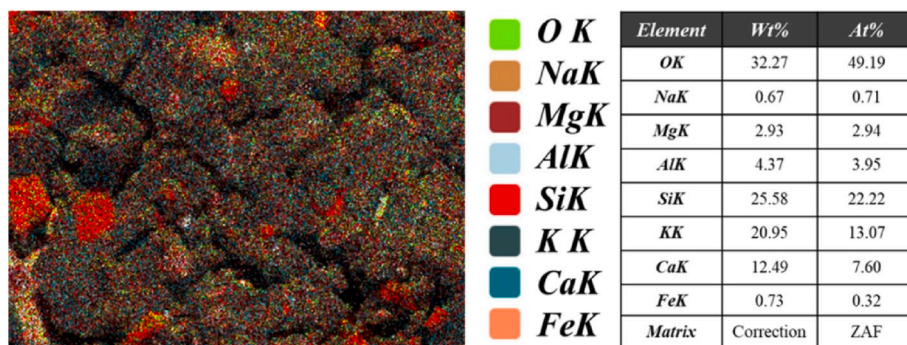

Element	Wt%	At%
OK	32.27	49.19
NaK	0.67	0.71
MgK	2.93	2.94
AlK	4.37	3.95
SiK	25.58	22.22
KK	20.95	13.07
CaK	12.49	7.60
FeK	0.73	0.32
Matrix	Correction	ZAF

Fig. 21. Element analysis of geopolymer.

as well as stability of nano-additive dispersions.

4. Conclusion

This work indicates that nanomaterials have the ability to contribute in geopolymer structure, showing improved mechanical properties and modified structure.

- Findings from this work have shown that nanomaterials have significantly enhanced the pumping time of the neat geopolymer slurry. Results showed that nano-additives increase the thickening time to 3 hrs at 50 °C and 14.7 MPa.
- Nanomaterials have increased the viscosity of the geopolymer slurry.

- MWCNT-OH decreased the fluid loss of the geopolymer. However, AL-0450 increases fluid loss compared to neat geopolymer.
- AL-0450 and MWCNT-OH both increased the compressive strength of the neat geopolymer from to 2945 psi to 4154 psi and 4274 psi respectively after 28 days.
- Stress strain curves showed better load carrying capacity and deformation for AL-0450 and MWCNT-OH based mixtures. However, after 28 days, mixtures become less ductile.
- Nanomaterials based mixtures did not show a significant increase in Young's modulus values compared to the neat geopolymer. AL-0450 showed more increase in Young's modulus after 3 days, due to high compressive strength.
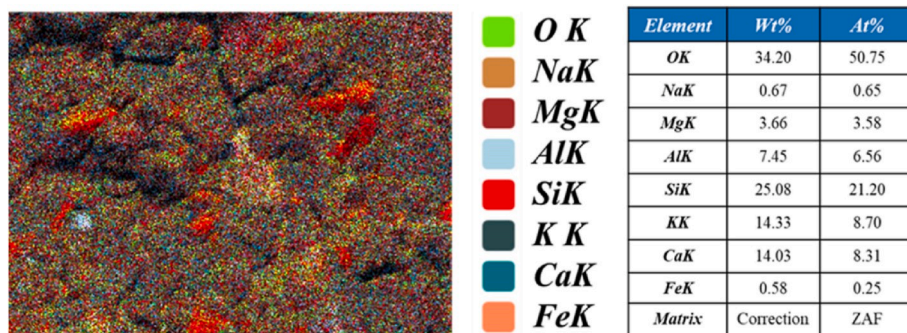
Element	Wt%	At%
OK	34.20	50.75
NaK	0.67	0.65
MgK	3.66	3.58
AlK	7.45	6.56
SiK	25.08	21.20
KK	14.33	8.70
CaK	14.03	8.31
FeK	0.58	0.25
Matrix	Correction	ZAF

Fig. 22. Element analysis of geopolymer with AL-0450 NPs.

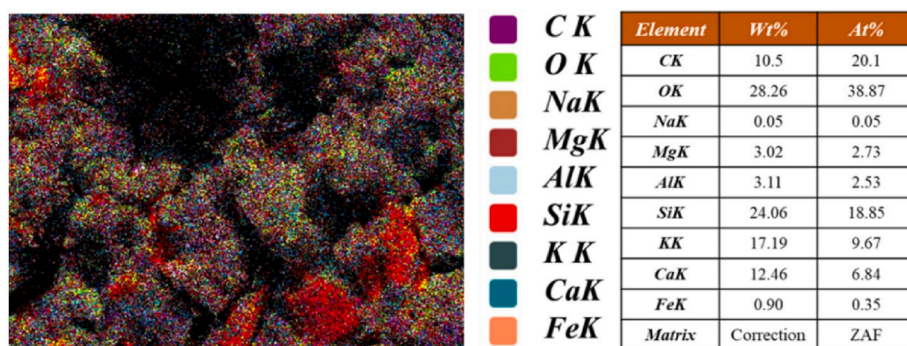| Element	Wt%	At%
CK	10.5	20.1
OK	28.26	38.87
NaK	0.05	0.05
MgK	3.02	2.73
AlK	3.11	2.53
SiK	24.06	18.85
KK	17.19	9.67
CaK	12.46	6.84
FeK	0.90	0.35
Matrix	Correction	ZAF

Fig. 23. Element analysis of geopolymer with MWCNT-OH particles.

- AL-0450 and MWCNT-OH based mixtures slightly increase the ratio of UCS and E after 28 days.
- In case of tensile strength, both AL-0450 and MWCNT-OH based mixtures showed improvement after 7 days. However, after 28 days, the increase is not very significant in case of AL-0450, while MWCNT-OH based mixture still showed improvement compared to neat geopolymer.
- Incorporation of nanomaterials produced a more flexible geopolymer structure until 7 days, with a significant increase in the tensile strength to Young's modulus ratio compared to neat geopolymer. However, after 28 days, tensile strength to Young's modulus for AL-0450 slightly decreases compared to neat geopolymer, while for MWCNT-OH ratio is improved compared to neat geopolymer, but decreases compared to 7 days.
- UCA results confirm the maximum strength development occurs at the early stages of curing.
- The XRD analysis showed the formation of new minerals that was an indication of the chemical reaction of nanoparticles with geopolymers.
- Dense and compact microstructure formation with the nanomaterials is being confirmed from the SEM analysis. Moreover, elemental analysis indicates the uniform distribution of nanomaterials in the geopolymer structure.
- This study indicates that nanomaterials can produce geopolymer material with improved mechanical strength and flexibility for a curing period of 7 days, however, for longer curing periods, nanomaterials might lose these properties as observed in this work. Therefore, future work should investigate the ability of nanomaterials to provide long term integrity.

Declaration of competing interest

The authors declare that they have no known competing financial interests or personal relationships that could have appeared to influence the work reported in this paper.

CRediT authorship contribution statement

Muhammad Awais Ashfaq Alvi: Conceptualization, Methodology, Investigation, Data curation, Writing - original draft, Writing - review & editing. **Mahmoud Khalifeh:** Conceptualization, Methodology, Writing - review & editing, Investigation, Resources, Supervision. **Mesfin Belayneh Agonafir:** Conceptualization, Supervision, Project administration, Funding acquisition.

Appendix A. Supplementary data

Supplementary data to this article can be found online at https://doi.org/10.1016/j.petrol.2020.107128.

References

Abbasi, S.M., Ahmadi, H., Khalaj, G., Ghasemi, B., 2016. Microstructure and mechanical properties of a metakaolinite-based geopolymer nanocomposite reinforced with carbon nanotubes. Ceram. Int. https://doi.org/10.1016/j.ceramint.2016.06.080.

Allouche, E., Lvov, Y., Montes, C., Joshi, A., 2017. Geopolymer with Nanoparticle Retardant and Method.

API, R.P., 2013. 10B-2: recommended practice for testing well cements. API Recomm. Pract. B 10.

Assaedi, H., Shaikh, F.U.A., Low, I.M., 2016. Effect of nano-clay on mechanical and thermal properties of geopolymer. J. Asian Ceram. Soc. https://doi.org/10.1016/j.jascer.2015.10.004.

Assaedi, H., Shaikh, F.U.A., Low, I.M., 2015. Utilization of nanoclay to reinforce flax fabric-geopolymer composites. Int. J. Chem. Mol. Nucl. Mater. Metall. Eng.

ASTM, C., 2013. Standard test method for compressive strength of hydraulic cement mortars (using 2-in. or [50-mm] cube specimens). Annu. B. ASTM Stand. B. ASTM Stand. 4, 1–9.

Belayneh, M., Aadnøy, B.S., 2015. Effect of nano and micro sized particle additives on the mechanical strength of cement plug. In: Proceedings of the International Conference on Offshore Mechanics and Arctic Engineering - OMAE. https://doi.org/10.1115/OMAE201541756.

Carragher, P.J., Fulks, J., 2018. Well abandonment solutions utilizing bismuth and thermite. In: Proceedings of the Annual Offshore Technology Conference.

Chindaprasirt, P., De Silva, P., Sagoe-Crentsil, K., Hanjitsuwan, S., 2012. Effect of SiO 2 and Al 2O 3on the setting and hardening of high calcium fly ash-based geopolymer systems. J. Mater. Sci. https://doi.org/10.1007/s10853-012-6353-y.

Davidovits, J., 2005. Geopolymer, Green Chemistry and Sustainable Development Solutions Chimie Verte et Solutions, Geopolymer chemistry and sustainable Development. The Poly(sialate) terminology : a very useful and simple model for the promot ion and understanding of green-chemistry.

Davidovits, J., 1991. Geopolymers - inorganic polymeric new materials. J. Therm. Anal. https://doi.org/10.1007/BF01912193.

Davidovits, J., 1982. Mineral Polymer and Methods of Making Them. United States Pat. U.S Patent No 4,349,386. https://patents.google.com/patent/US4349386A/en.

De Andrade, J., Sangesland, S., 2016. Cement sheath failure mechanisms: numerical estimates to design for long-term well integrity. J. Pet. Sci. Eng. https://doi.org/10.1016/j.petrol.2016.08.032.

de Paula, J.N., Calixto, J.M., Ladeira, L.O., Ludvig, P., Souza, T.C.C., Rocha, J.M., de Melo, A.A.V., 2014. Mechanical and rheological behavior of oil-well cement slurries produced with clinker containing carbon nanotubes. J. Pet. Sci. Eng. https://doi.org/10.1016/j.petrol.2014.07.020.

Deb, P.S., Sarker, P.K., Barbhuiya, S., 2016. Sorptivity and acid resistance of ambient-cured geopolymer mortars containing nano-silica. Cem. Concr. Compos. https://doi.org/10.1016/j.cemconcomp.2016.06.017.

Duxson, P., Fernández-Jiménez, A., Provis, J.L., Lukey, G.C., Palomo, A., Van Deventer, J.S.J., 2007. Geopolymer technology: the current state of the art. J. Mater. Sci. https://doi.org/10.1007/s10853-006-0637-z.

Ershadi, V., Ebadi, T., Rabani, A., Ershadi, L., Soltanian, H., 2013. The effect of nanosilica on cement matrix permeability in oil well to decrease the pollution of receptive environment. Int. J. Environ. Sci. Dev. https://doi.org/10.7763/ijesd.2011.v2.109.

Gao, K., Lin, K.-L., Wang, D., Shiu, H.-S., Hwang, C.-L., Cheng, T.-W., 2013. Effects of nano-SiO2 on setting time and compressive strength of alkaliactivated metakaolin-based geopolymer. Open Civ. Eng. J. https://doi.org/10.2174/1874149501307010084.

Gao, K., Lin, K.L., Wang, D., Hwang, C.L., Shiu, H.S., Chang, Y.M., Cheng, T.W., 2014. Effects SiO2/Na2O molar ratio on mechanical properties and the microstructure of nano-SiO2 metakaolin-based geopolymers. Constr. Build. Mater. https://doi.org/10.1016/j.conbuildmat.2013.12.003.

Guo, X., Hu, W., Shi, H., 2014. Microstructure and self-solidification/stabilization (S/S) of heavy metals of nano-modified CFA-MSWIFA composite geopolymers. Constr. Build. Mater. https://doi.org/10.1016/j.conbuildmat.2014.01.062.

Hajimohammadi, A., Ngo, T., Mendis, P., 2017. How does aluminium foaming agent impact the geopolymer formation mechanism? Cem. Concr. Compos. https://doi.org/10.1016/j.cemconcomp.2017.03.022.

Hassaan, M.M., Khater, H.M., El-Mahllawy, M.S., El Nagar, A.M., 2015. Production of geopolymer composites enhanced by nano-kaolin material. J. Adv. Ceram. https://doi.org/10.1007/s40145-015-0156-y.

Hodne, H., Saasen, A., Strand, S., 2001. Rheological properties of high temperature oil well cement slurries. In: Annual Transactions of the Nordic Rheology Society.

Huang, Y., Han, M., 2011. The influence of α-Al2O3 addition on microstructure, mechanical and formaldehyde adsorption properties of fly ash-based geopolymer products. J. Hazard. Mater. https://doi.org/10.1016/j.jhazmat.2011.07.029.

Jafariesfad, N., Geiker, M.R., Gong, Y., Skalle, P., Zhang, Z., He, J., 2017a. Cement sheath modification using nanomaterials for long-term zonal isolation of oil wells: Review. J. Pet. Sci. Eng. https://doi.org/10.1016/j.petrol.2017.06.047.

Jafariesfad, N., Khalifeh, M., Skalle, P., Geiker, M.R., 2017b. Nanorubber-modified cement system for oil and gas well cementing application. J. Nat. Gas Sci. Eng. https://doi.org/10.1016/j.jngse.2017.10.002.

Jalal, M., Mansouri, E., Sharifipour, M., Pouladkhan, A.R., 2012. Mechanical, rheological, durability and microstructural properties of high performance self-compacting concrete containing SiO 2 micro and nanoparticles. Mater. Des. https://doi.org/10.1016/j.matdes.2011.08.037.

Khalifeh, M., Hodne, H., Korsnes, R.I., Saasen, A., 2015. Cap Rock Restoration in Plug and Abandonment Operations; Possible Utilization of Rock-Based Geopolymers for Permanent Zonal Isolation and Well Plugging. https://doi.org/10.2523/iptc-18454-ms.

Khalifeh, M., Hodne, H., Saasen, A., Vralstad, T., 2013. Techniques and Materials for North Sea Plug and Abandonment Operations. https://doi.org/10.4043/23915-ms.

Khalifeh, M., Saasen, A., Hodne, H., Godøy, R., Vrålstad, T., 2018. Geopolymers as an alternative for oil well cementing applications: a review of advantages and concerns. J. Energy Resour. Technol. https://doi.org/10.1115/1.4040192.

Khalifeh, M., Saasen, A., Hodne, H., Motra, H.B., 2019a. Laboratory evaluation of rock-based geopolymers for zonal isolation and permanent P&A applications. J. Pet. Sci. Eng. https://doi.org/10.1016/j.petrol.2018.12.065.

Khalifeh, M., Saasen, A., Vralstad, T., Hodne, H., 2014. Potential utilization of class C fly ash-based geopolymer in oil well cementing operations. Cem. Concr. Compos. https://doi.org/10.1016/j.cemconcomp.2014.06.014.

Khalifeh, M., Saasen, A., Vrålstad, T., Larsen, H.B., Hodne, H., 2016. Experimental study on the synthesis and characterization of aplite rock-based geopolymers. J. Sustain. Cem. Mater. https://doi.org/10.1080/21650373.2015.1044049.

Khalifeh, M., Salehi, S., Jamrozik, A., Kimanzi, R., Abdollahpour, S., 2019b. Nano-modified rock-based geopolymers as supplement to Portland cement for oil well cementing. In: Proceedings of the International Conference on Offshore Mechanics and Arctic Engineering.

Khalifeh, M., Todorovic, J., Vrålstad, T., Saasen, A., Hodne, H., 2017. Long-term durability of rock-based geopolymers aged at downhole conditions for oil well cementing operations. J. Sustain. Cem. Mater. https://doi.org/10.1080/21650373.2016.1196466.

Khan, W.A., Rahman, M.K., Mahmoud, M.A., Sarmah, P., 2016. MWCNT for Enhancing Mechanical Properties of Oil Well Cement for HPHT Applications. https://doi.org/10.2118/178175-ms.

Khater, H.M., Abd El Gawaad, H.A., 2016. Characterization of alkali activated geopolymer mortar doped with MWCNT. Constr. Build. Mater. https://doi.org/10.1016/j.conbuildmat.2015.10.121.

Kiran, R., Teodoriu, C., Dadmohammadi, Y., Nygaard, R., Wood, D., Mokhtari, M., Salehi, S., 2017. Identification and evaluation of well integrity and causes of failure of well integrity barriers (A review). J. Nat. Gas Sci. Eng. 45, 511–526. https://doi.org/10.1016/j.jngse.2017.05.009. https://www.sciencedirect.com/science/article/pii/S1875510017302184#!.

Komnitsas, K.A., 2011. Potential of geopolymer technology towards green buildings and sustainable cities. In: Procedia Engineering. https://doi.org/10.1016/j.proeng.2011.11.2108.

Lavrov, A., Torsæter, M., n.d. Physics and Mechanics of Primary Well Cementing. Springer.

Leiva, C., Luna-Galiano, Y., Arenas, C., Alonso-Fariñas, B., Fernández-Pereira, C., 2019. A porous geopolymer based on aluminum-waste with acoustic properties. Waste Manag. https://doi.org/10.1016/j.wasman.2019.06.042.

Li, H., Xiao, H. gang, Ou, J. ping, 2004. A study on mechanical and pressure-sensitive properties of cement mortar with nanophase materials. Cem. Concr. Res. https://doi.org/10.1016/j.cemconres.2003.08.025.

Li, M., Deng, S., Meng, F., Hao, J., Guo, X., 2017. Effect of nanosilica on the mechanical properties of oil well cement at low temperature. Mag. Concr. Res. https://doi.org/10.1680/jmacr.16.00394.

Li, Z., Chen, R., Zhang, L., 2013. Utilization of chitosan biopolymer to enhance fly ash-based geopolymer. J. Mater. Sci. https://doi.org/10.1007/s10853-013-7610-4.

Liu, X., 2017. Mud-to-cement conversion of synthetic-based drilling muds using geopolymers (Doctoral Dissertation) Retrieved from. https://repositories.lib.utexas.edu/handle/2152/63651.

Liu, X., Ramos, M.J., Nair, S.D., Lee, H., Espinoza, D.N., van Oort, E., 2017. True Self-Healing Geopolymer Cements for Improved Zonal Isolation and Well Abandonment. https://doi.org/10.2118/184675-ms.

Lo, K.W., Lin, K.L., Cheng, T.W., Chang, Y.M., Lan, J.Y., 2017. Effect of nano-SiO2 on the alkali-activated characteristics of spent catalyst metakaolin-based geopolymers. Constr. Build. Mater. https://doi.org/10.1016/j.conbuildmat.2017.03.152.

Meng, T., Yu, Y., Qian, X., Zhan, S., Qian, K., 2012. Effect of nano-TiO 2 on the mechanical properties of cement mortar. Constr. Build. Mater. https://doi.org/10.1016/j.conbuildmat.2011.10.047.

Murtaza, M., Rahman, M.K., Al-Majed, A.A., 2016. Effect of Nanoclay on Mechanical and Rheological Properties of Oil Well Cement Slurry under HPHT Environment. https://doi.org/10.2523/iptc-18989-ms.

Naskar, S., Chakraborty, A.K., 2016. Effect of nano materials in geopolymer concrete. Perspect. Sci. https://doi.org/10.1016/j.pisc.2016.04.049.

Nasvi, M.C.M., Ranjith, P.G., Sanjayan, J., Bui, H., 2014. Effect of temperature on permeability of geopolymer: a primary well sealant for carbon capture and storage wells. Fuel. https://doi.org/10.1016/j.fuel.2013.09.007.

Nelson, D.G.E.B., Guillot, D., 2006. Well Cementing, second ed. Schlumberger, Sugar land, Texas.

Norsok, D., 2013. 010. Well integrity in drilling and well operations. Stand. Norway. Rev 4.

Norway, P., 2019. PSA - RNNP Presentation 2019 [WWW Document]. Well Integr. Semin. 2019. https://www.norskoljeoggass.no/contentassets/61f374c11c854015bc45f7be3f9b51c0/psa—rnnp-presentasjon-2019_wif-seminar-13.6.2019-til-wif—without-film.pdf.

Norway, S., 2009. NS-EN 12390-6:2009 Testing Hardened Concrete - Part 6:Tensile Splitting Strength of Test Specimens.

Norway, S., 2005. NS-EN 196-1: Methods of Testing Cement Part 1 (Determination of strength).

Ochoa, M.V., 2006. Analysis of Drilling Fluid Rheology and Tool Joint Effect to Reduce Errors in Hydraulics Calculations. Texas A&M University.

Ozyildirim, C., Zegetosky, C., 2010. Exploratory investigation of nanomaterials to improve strength and permeability of concrete. Transp. Res. Rec. J. Transp. Res. Board. https://doi.org/10.3141/2142-01.

Paiva, M.D.M., Silva, E.C.C.M., Melo, D.M.A., Martinelli, A.E., Schneider, J.F., 2018. A geopolymer cementing system for oil wells subject to steam injection. J. Pet. Sci. Eng. https://doi.org/10.1016/j.petrol.2018.06.022.

Panchmatia, P., Zhou, N.S., Juenger, M., van Oort, E., 2019. Monitoring the strength development of alkali-activated materials using an ultrasonic cement analyzer. J. Pet. Sci. Eng. https://doi.org/10.1016/j.petrol.2019.05.070.

Pang, X., Boul, P.J., Cuello Jimenez, W., 2014. Nanosilicas as accelerators in oilwell cementing at low temperatures. SPE Drill. https://doi.org/10.2118/168037-pa. Complet.

Phoo-ngernkham, T., Chindaprasirt, P., Sata, V., Hanjitsuwan, S., Hatanaka, S., 2014. The effect of adding nano-SiO2 and nano-Al2O3 on properties of high calcium fly ash geopolymer cured at ambient temperature. Mater. Des. https://doi.org/10.1016/j.matdes.2013.09.049.

Provis, J.L., Van Deventer, J.S.J., 2009. Geopolymers: Structures, Processing, Properties and Industrial Applications, Geopolymers: Structures, Processing, Properties and Industrial Applications. https://doi.org/10.1533/9781845696382.

Riahi, S., Nazari, A., 2012. The effects of nanoparticles on early age compressive strength of ash-based geopolymers. Ceram. Int. https://doi.org/10.1016/j.ceramint.2012.02.021.

Ridha, S., Yerikania, U., 2015. The Strength Compatibility of Nano-SiO2 Geopolymer cement for oil well under HPHT conditions. J. Civ. Eng. Res. 5, 6–10.

Rodríguez, E.D., Bernal, S.A., Provis, J.L., Paya, J., Monzo, J.M., Borrachero, M.V., 2013. Effect of nanosilica-based activators on the performance of an alkali-activated fly ash binder. Cem. Concr. Compos. https://doi.org/10.1016/j.cemconcomp.2012.08.025.

Rovnaník, P., Šimonová, H., Topolář, L., Schmid, P., Keršner, Z., 2016. Effect of carbon nanotubes on the mechanical fracture properties of fly ash geopolymer. In: Procedia Engineering. https://doi.org/10.1016/j.proeng.2016.07.360.

Roy-Delage, L., Baumgarte, C., Thiercelin, M., Vidick, B., 2000. New cement systems for durable zonal isolation. In: IADC/SPE Drilling Conference. Society of Petroleum Engineers.

Saafi, M., Andrew, K., Tang, P.L., McGhon, D., Taylor, S., Rahman, M., Yang, S., Zhou, X., 2013. Multifunctional properties of carbon nanotube/fly ash geopolymeric nanocomposites. Constr. Build. Mater. https://doi.org/10.1016/j.conbuildmat.2013.08.007.

Saasen, A., Ytrehus, J.D., 2018. Rheological properties of drilling fluids: use of dimensionless shear rates in Herschel-Bulkley and power-law models. Appl. Rheol. https://doi.org/10.3933/applrheol-28-54515.

Safi, B., Aknouche, H., Mechakra, H., Aboutaleb, D., Bouali, K., 2018. Incorporation mode effect of Nano-silica on the rheological and mechanical properties of cementitious pastes and cement mortars. In: IOP Conference Series: Earth and Environmental Science. https://doi.org/10.1088/1755-1315/143/1/012015.

Salehi, S., Ali, N., Khattak, M.J., Rizvi, H., 2016. Geopolymer Composites as Efficient and Economical Plugging Materials in Peanuts Price Oil Market. https://doi.org/10.2118/181426-ms.

Salehi, S., Khattak, J., Saleh, F.K., Igbojekwe, S., 2019. Investigation of mix design and properties of geopolymers for application as wellbore cement. J. Pet. Sci. Eng. https://doi.org/10.1016/j.petrol.2019.03.031.

Salehi, S., Khattak, M.J., Ali, N., Ezeakacha, C., Saleh, F.K., 2017. Study and use of geopolymer mixtures for oil and gas well cementing applications. J. Energy Resour. Technol. https://doi.org/10.1115/1.4037713.

Shenold, C., Teodoriu, C., 2016. Development of a structured workflow for enhanced well cement integrity: lessons learned and the way ahead. J. Nat. Gas Sci. Eng. https://doi.org/10.1016/j.jngse.2016.10.042.

Singh, B., Ishwarya, G., Gupta, M., Bhattacharyya, S.K., 2015. Geopolymer concrete: a review of some recent developments. Constr. Build. Mater. https://doi.org/10.1016/j.conbuildmat.2015.03.036.

Standard, A., n.d. D3967-16 (2016) Standard Test Method for Splitting Tensile Strength of Intact Rock Core Specimens. ASTM Int. West Conshohocken, USA.

Sumesh, M., Alengaram, U.J., Jumaat, M.Z., Mo, K.H., Alnahhal, M.F., 2017. Incorporation of nano-materials in cement composite and geopolymer based paste and mortar – a review. Constr. Build. Mater. https://doi.org/10.1016/j.conbuildmat.2017.04.206.

Teodoriu, C., Kosinowski, C., Amani, M., Schubert, J., Shadravan, A., 2013. Wellbore integrity AND cement failure at hpht conditions. Int. J. Eng. Appl. Sci.

Thiercelin, M.J., Dargaud, B., Baret, J.F., Rodriquez, W.J., 1998. Cement design based on cement mechanical response. SPE Drill. Complet. 13, 266–273.

Vignes, B., Aadnøy, B.S., 2010. Well-integrity issues offshore Norway. In: SPE Production and Operations. https://doi.org/10.2118/112535-PA.

Vrålstad, T., Saasen, A., Fjær, E., Øia, T., Ytrehus, J.D., Khalifeh, M., 2018. Plug & abandonment of offshore wells: ensuring long-term well integrity and cost-efficiency. J. Pet. Sci. Eng.

Watson, T.L., Bachu, S., 2009. Evaluation of the potential for gas and CO2 leakage along wellbores. SPE Drill. Complet. https://doi.org/10.2118/106817-pa.

Williams, R.H., Khatri, D.K., Keese, R.F., Le Roy-Delage, S., Roye, J.M., Leach, D.L.R., Porcherie, O., Rottler, P., Rodriguez, J., 2011. Flexible, Expanding Cement System (FECS) Successfully Provides Zonal Isolation across Marcellus Shale Gas Trends. https://doi.org/10.2118/149440-ms.

Yang, L.Y., Jia, Z.J., Zhang, Y.M., Dai, J.G., 2015. Effects of nano-TiO2 on strength, shrinkage and microstructure of alkali activated slag pastes. Cem. Concr. Compos. https://doi.org/10.1016/j.cemconcomp.2014.11.009.

Yong, S.L., Feng, D.W., Lukey, G.C., van Deventer, J.S.J., 2007. Chemical characterisation of the steel-geopolymeric gel interface. Colloids Surfaces A Physicochem. Eng. Asp. https://doi.org/10.1016/j.colsurfa.2007.03.004.